Statistics of the structure components in S0s: implications for bar-induced secular evolution

E. Laurikainen,[1,2]⋆ H. Salo,[1] E. Athanassoula,[3] A. Bosma,[3] R. Buta[4] and J. Janz[1,5]

[1]*Department of Physics/Astronomy Division, University of Oulu, FI-90014 Finland*
[2]*Finnish Centre of Astronomy with ESO (FINCA), University of Turku, Väisäläntie 20, FI-21500, Piikkiö, Finland*
[3]*Aix Marseille Université, CNRS, LAM (Laboratoire d'Astrophysique de Marseille) UMR 7326, 13388, Marseille, France*
[4]*Department of Physics and Astronomy, University of Alabama, Box 870324, Tuscaloosa, AL 35487, USA*
[5]*Astronomisches Rechen-Institut, Zentrum für Astronomie der Universität Heidelberg, Mönchhofstrase 12-14, D-69120 Heidelberg, Germany*

ABSTRACT

The fractions and dimension of bars, rings and lenses are studied in the near-infrared (IR) S0 galaxy survey, which is a sample of ∼200 early-type disc galaxies, mainly S0s. We find evidence that multiple lenses in some barred S0s are related to bar resonances in a similar manner as the inner and outer rings, for which the outer/inner length ratio is ∼2. Inner lenses in the non-barred galaxies normalized to galaxy diameter are clearly smaller than those in the barred systems. Interestingly, these small lenses in the non-barred galaxies have similar sizes as barlenses (lens-like structures embedded in a bar), and therefore might actually be barlenses in former barred galaxies, in which the outer, more elongated bar component has been destroyed. We also find that fully developed inner lenses are on average a factor of 1.3 larger than bars, whereas inner rings have similar sizes as bars. The fraction of inner lenses is found to be constant in all family classes (A, AB, B). Nuclear bars appear most frequently among the weakly barred (AB) galaxies, which are consistent with the theoretical models by Maciejewski & Athanassoula. Similar-sized bars as the nuclear bars were detected in seven 'non-barred' S0s. Galaxy luminosity does not uniquely define the sizes of bars or bar-related structures, neither is there any upper limit in galaxy luminosity for bar formation. Although all the family classes cover the same range of galaxy luminosity, the non-barred (A) galaxies are on average 0.6 mag brighter than the strongly barred (B) systems. Overall, our results are consistent with the idea that bars play an important role in the formation of the structure components of galaxies. The fact that multiple lenses are common in S0s, and that at least the inner lenses can have very old stellar populations, implies that the last destructive merger or major gas accretion event, must have taken place at a fairly high redshift.

Key words: galaxies: elliptical and lenticular, cD – galaxies: evolution – galaxies: statistics – galaxies: structure.

1 INTRODUCTION

Galaxy morphology is a subject of significant recent turmoil, both theoretically and observationally. The early-type disc galaxies have an important role in this debate. In the current paradigm of galaxy formation (White & Rees 1978; Frenk et al. 1985), morphology at high redshifts is a transient property changing between spirals and ellipticals, e.g. discs are renovated after each merger event, unless the gas in the halo becomes too hot for participating in the disc rebuilding anymore. After the merger-dominated era, intrinsic secular dynamical evolution is expected to play an increasing role. A different view is taken by Sales et al. (2013) who suggested that most stars in bulges and discs form in situ from hot and cold gas falling in from the halo. In that case, no correlation is expected between the stellar population ages and the epochs of the formation of structures in galaxies.

Even within the standard picture of galaxy evolution there is an active debate of how important secular evolution is in the formation of structures of local galaxies, when did the secular processes start to dominate and what are the driving forces of that evolution. It has been suggested (Hammer et al. 2009; Puech et al. 2012) that

⋆ E-mail: eija.laurikainen@oulu.fi

even up to 50 per cent of the spiral galaxy discs might have been formed via disc rebuilding soon after the most recent merger event. On the other hand, dynamical evolution can be largely driven by bars (Sellwood & Wilkinson 1993; Kormendy & Kennicutt 2004; Hopkins et al. 2010; Athanassoula 2012), without invoking any significant gas accretion. One important problem in the present-day cosmological simulations is that disc galaxies with excessive B/T flux-ratios and too large values of the Sérsic index are created (Navarro & Benz 1991), unless the galaxies have extremely quiescent merger and gas-accretion histories (Kraljic, Bournaud & Martig 2011; Martig et al. 2012). Disc-like bulges (low Sérsic index) are created also in cosmological simulations by starbursts at high redshifts, but those bulges are still very massive compared to typically observed bulges (Wang et al. 2011; Okamoto 2013). In non-cosmological simulations, where it is possible to study a controlled range of various parameters, the problem of massive bulges can be avoided if the galaxies evolve in very dense environments (Khochfar et al. 2011), or if two gas rich pure disc galaxies are made to merge (Keselman & Nusser 2012). However, a large majority of the S0s in the local Universe have low B/T flux-ratios; moreover their Sérsic indexes are close to 1–2 indicating that the bulges are fairly exponential (Laurikainen et al. 2005, 2010). In cosmological simulations discs are easily destroyed by infalling satellites (Toth & Ostriker 1992) or by accretion of misaligned gas (Scannapieco et al. 2009; Sales et al. 2013), which is challenging when explaining the observed large-scale lenses in many S0 galaxies.

Lower B/T flux-ratios and longer lasting disc structures are expected if galaxy evolution after $z \sim 1$ was mostly quiescent. In that case, the S0s could be largely red and dead (or at most partly re-rejuvenated) former spirals in which the gas does not participate in the disc rebuilding anymore. Strong support for this comes from the recently suggested scenario, in which the S0s form a parallel sequence with the spirals in the Hubble diagram (Laurikainen et al. 2010; Cappellari et al. 2011; Kormendy & Bender 2012), renovating the old idea of van den Bergh (1976). In that scenario, both the early and late-type spirals evolve directly into S0s forming S0a, S0b and S0c types. This makes it possible to understand the observed small B/T flux-ratios in some S0s and also why the properties of the bulges and discs are so similar in the S0s and spirals (Laurikainen et al. 2010). Motivated by the fact that as much as 70 per cent of the S0s live in galaxy groups (Wilmann et al. 2009; Just et al. 2011), Eliche-Moral et al. (2012) suggested that the transformation from spirals into S0s could occur via minor mergers, leading to the observed parallel sequence, provided that the bulges were originally very small disc-like components. Bars might also be a driving force in the transformation process, though that has not been studied in detail yet.

Understanding the formation of bars, lenses and rings is important, and it is not yet clear what exactly they mean for galaxy dynamics and evolution (see review by Buta 2013). The least well understood are the lenses, which are morphological components with a shallow brightness gradient interior to a sharp edge. One formation process suggested for the lenses in the S0s is that they are formed via bar dissolution, finally ending up to nearly axisymmetric structures (Kormendy 1979). However, this cannot be the whole story, because more than one type of lenses (nuclear, inner and outer) exist, and often multiple lenses are found in the same galaxies (Kormendy 1979; Laurikainen et al. 2011). Alternatively, lenses can form via disc instability in a similar manner as bars (Athanassoula 1983), or via truncated star formation in the distant past (Bosma 1983). However, none of the above processes are capable of explaining multiple lenses in S0s, of which a pictorial example is NGC 1411 (Laurikainen et al. 2006; Buta et al. 2007). Recently, a new lens-type, a *barlens*, was recognized by Laurikainen et al. (2011), identified as a distinct rounder component in the inner part of a bar. If barlenses form part of the bar, this opens a new angle for understanding bars and lenses in galaxy evolution, which will be discussed in this study.

In order to study possible manifestations of secular evolution in galaxy morphology, statistics of the structural components are compiled and the dimensions of the structures are studied for a sample of ∼200 early-type disc galaxies, mainly S0s. We find that bars are important drivers of secular evolution in galaxies. In particular, a new explanation for the formation of inner lenses in the non-barred galaxies is suggested.

2 THE DATA BASE

As a data base, we use the near-infrared (IR) S0 galaxy survey (hereafter NIRS0S Atlas; Laurikainen et al. 2011), which is a magnitude ($m_B \leq 12.5$ mag) and inclination-limited (less than $65°$) sample of ∼200 early-type disc galaxies, including 160 S0+S0/a galaxies, 33 Sa spirals and 12 late-type ellipticals.[1] The K_s-band images typically reach a surface brightness of 23.5 mag arcsec^{-2} in azimuthally averaged profiles, being 2–3 mag deeper than the 2 Micron All Sky Survey (2MASS[2]) images. In this study, we use the new morphological classifications of the NIRS0S Atlas, where also the measurements of the dimensions of the structures are given.

The morphological classification is based on the de Vaucouleurs' revised Hubble–Sandage system, but is more detailed than that. It includes the stage (S0$^-$, S0°, S0$^+$, Sa), family (SA, SAB, SB), variety (r, rs, s), outer ring or pseudo-ring (R, R$'$), possible spindle shape and the presence of peculiarity. Lenses (nuclear, inner, outer) are systematically coded in a similar manner as in Kormendy (1979) and in Buta et al. (2010). The classification distinguishes ansae and x-shaped bars from regularly shaped bar morphologies. Also, due to the sub-arcsecond pixel resolution, it was possible to classify central structures like nuclear bars, rings and lenses in a systematic manner. The NIRS0S Atlas also includes the identification of weak bars in the residual images, after subtracting the bulge model, obtained from the structural decompositions. Alternatively, weak structures were detected in unsharp mask images (a smoothed image subtracted from the original image). These faint structures, together with the identification of an exponential outer surface brightness profiles, form part of the photometric classification given in the NIRS0S Atlas, which is generally used in this study. Examples of the Atlas galaxies are shown in Fig. 1.

Included in the analysis are also the photometric properties of bulges, obtained for the same galaxies by Laurikainen et al. (2010), based on two-dimensional multicomponent structural decompositions.[3] In the decompositions, analytical functions

---

[1] These numbers include 29 galaxies with $12.5 < m_B < 12.7$, which strictly speaking do not belong to the magnitude-limited sample. However, none of the results reported below would change if they are omitted from the statistics.

[2] 2MASS is a joint project of the University of Massachusetts and the Infrared Processing and Analysis Center/California Institute of Technology, funded by the National Aeronautics and Space Administration and the National Science Foundation.

[3] The decompositions were performed with the BDBAR code (Laurikainen et al. 2004, 2005), written by Salo.
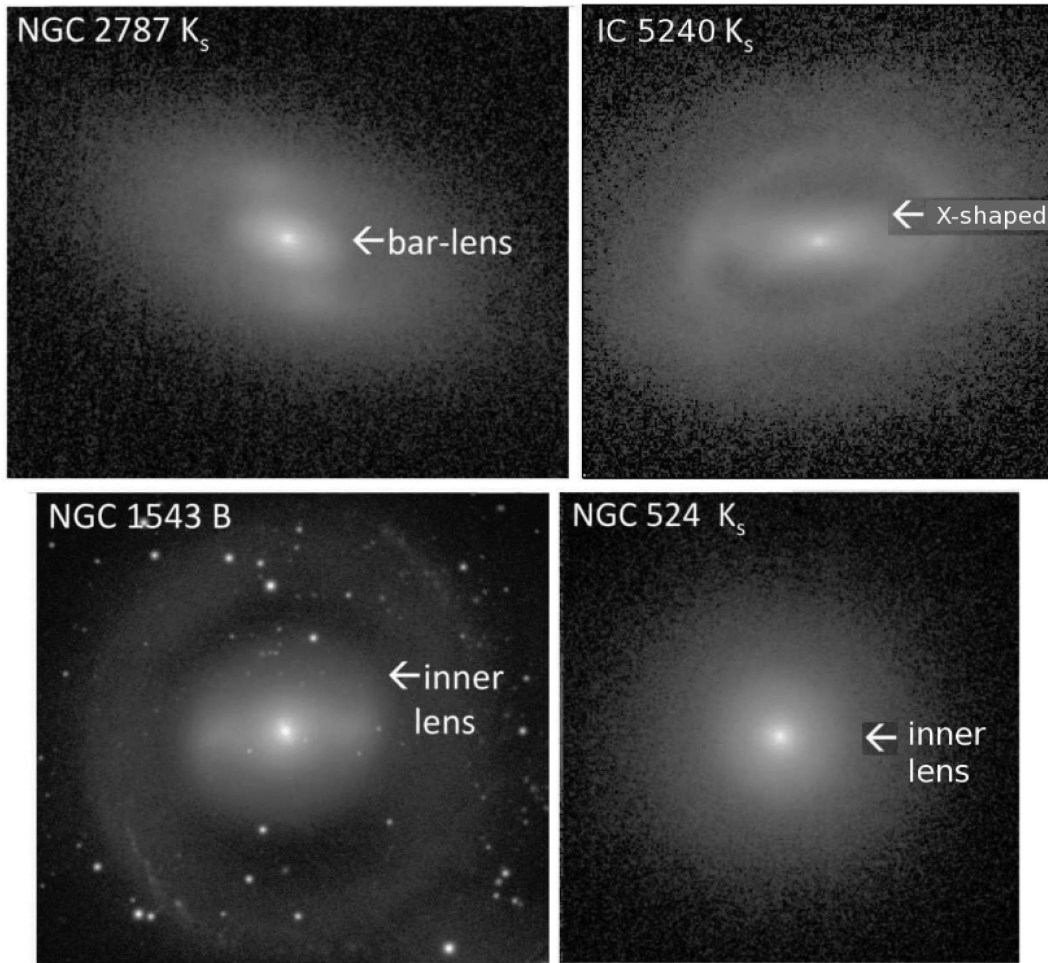
Figure 1. Galaxies from the NIRS0S Atlas (Laurikainen et al. 2011) demonstrating the different structure components. The images typically reach a surface brightness of 23.5 mag arcsec^{-2} in the K_s band, corresponding to a surface brightness of 27.5 mag arcsec^{-2} in the B band. The galaxies are shown in a magnitude scale.

(Sérsic, Ferrers, exponential) were fitted, in addition to the bulges and discs, also to bars (including nuclear bars), lenses and ovals.

2.1 Definitions of the structures in the classification

L, l, nl

By lenses we mean flat light distributions in the discs, with fairly sharp outer edges. Such structures form part of the original galaxy classification (Sandage 1961; Sandage & Bedke 1994), though no coding for the lenses was used at that time. Nuclear, inner and outer lenses are denoted by nl, l and L, respectively. In barred galaxies the inner lenses have sizes roughly similar to bars, whereas in non-barred galaxies the relative size compared to the galaxy size defines the subtype. Outer lenses are clearly larger than the inner lenses, and nuclear lenses are small central structures with similar sizes as the nuclear rings.

bl

Barlenses are lens-like structures embedded in the bars. In distinction to bulges they have much flatter light distributions, whereas in distinction to nuclear lenses they are much larger, typically covering 50 per cent of the bar size. Barlenses can be aligned with the main bar or be slightly twisted from the major axis orientation of the bar.

R, r, nr

Rings are structures in which both the inner and outer regions have well-defined edges. The rings can be full rings or non-complete pseudo-rings, of which both can further have their subtypes (see Buta 1995). Sometimes an inner ring is seen mainly because of dark space around the sides of the bar.

RL, rl, nrl

Ringlenses are intermediate types between rings and lenses. They have no well-defined inner edges, but the surface brightness increases towards the outer regions, until the light distribution drops, in a similar manner as in rings. Ringlenses are divided into nuclear, inner and outer structures (nrl, rl, RL) in a similar manner as rings. Ringlenses have also similar subtypes as rings.

2.2 Size measurements of the structures

In the NIRS0S Atlas, the sizes of the structures are given in the sky plane (tables 5 and 6 in the Atlas). The classified features were first inspected visually in the images. If a feature was a clear ring or ringlens, the cursor was used with IRAF routine TVMARK to outline the ridge line. If the feature was a lens, the outer edge was mapped instead. After that an ellipse-fitting program was used to

Table 1. Fractions of structure components in different Hubble types in the *complete NIRS0S* (S0−Sa). multi$_l$ contains full lenses, and multi$_{l,rl}$ contains both lenses and ringlenses. multi$_{bar}$ means galaxies with two or more bars identified visually, whereas multi$_{bar}$(res) includes also weak bars detected by other means. N_{tot} is the total galaxy number in each Hubble-type bin and the numbers for the different structure component are given in parenthesis. The Hubble types earlier than $T = -3$ are not shown.

Hubble stage: (N_{tot} in bin)	−3 (49)	−2 (40)	−1 (32)	0 (29)	1 (33)
Bars:					
A	63 ± 7% (31)	50 ± 8% (20)	16 ± 6% (5)	24 ± 8% (7)	18 ± 7% (6)
AB	20 ± 6% (10)	20 ± 6% (8)	41 ± 9% (13)	38 ± 9% (11)	51 ± 9% (17)
B	14 ± 5% (7)	30 ± 7% (12)	44 ± 9% (14)	38 ± 9% (11)	30 ± 8% (10)
B+AB	35 ± 7% (17)	50 ± 8% (20)	84 ± 6% (27)	76 ± 8% (22)	82 ± 7% (27)
multi$_{bar}$	6 ± 3% (3)	10 ± 5% (4)	22 ± 7% (7)	14 ± 6% (4)	9 ± 5% (3)
multi$_{bar}$(res)	10 ± 4% (5)	15 ± 6% (6)	37 ± 9% (12)	17 ± 7% (5)	21 ± 7% (7)
Lenses:					
L	26 ± 6% (13)	18 ± 6% (7)	9 ± 5% (3)	3 ± 3% (1)	3 ± 3% (1)
l	28 ± 6% (14)	25 ± 7% (10)	9 ± 5% (3)	14 ± 6% (4)	12 ± 6% (4)
nl	8 ± 4% (4)	20 ± 6% (8)	22 ± 7% (7)	21 ± 8% (6)	18 ± 7% (6)
bl	6 ± 3% (3)	18 ± 6% (7)	38 ± 9% (12)	24 ± 8% (7)	21 ± 7% (7)
multi$_l$	14 ± 5% (7)	15 ± 6% (6)	6 ± 4% (2)	7 ± 5% (2)	6 ± 4% (2)
L, RL	31 ± 7% (15)	35 ± 7% (14)	34 ± 8% (11)	34 ± 9% (10)	12 ± 6% (4)
RL	4 ± 2% (21)	18 ± 6% (7)	25 ± 7% (8)	31 ± 9% (9)	9 ± 5 (3)
l, rl	28 ± 6% (14)	40 ± 8% (16)	41 ± 9% (13)	28 ± 8% (8)	21 ± 7% (7)
rl	–	15 ± 6% (6)	31 ± 8% (10)	14 ± 6% (4)	9 ± 6% (3)
nl, rnl	10 ± 4% (5)	25 ± 7% (10)	25 ± 8% (8)	24 ± 8% (7)	18 ± 7% (6)
multi$_{l,rl}$	16 ± 5% (8)	30 ± 7% (12)	28 ± 8% (9)	24 ± 8% (7)	9 ± 5% (3)
Rings:					
Outer	–	5 ± 3% (2)	25 ± 8% (8)	21 ± 8% (6)	42 ± 9% (14)
Inner(r, rs)	2 ± 2% (1)	8 ± 4% (3)	28 ± 8% (9)	21 ± 8% (6)	15 ± 6% (5)
Nuclear	–	3 ± 3% (1)	25 ± 8% (8)	7 ± 5% (2)	12 ± 6% (4)

fit the points, which gave the centre coordinates, the position angle of the major axis, the major axis radius and the axis ratio of the component. For bars, the edge of the bar defined its size.

In this study, the size measurements given in the NIRS0S Atlas were converted to the plane of the galactic disc using the orientation parameters obtained from the apparent major axis position angle and the minor-to-major axis ratio, based on fitting ellipses to the outer isophotes. For the orientation parameters our deep optical (B,V) images were used when available, otherwise the K_s-band NIRS0S images were used.

3 FREQUENCY OF THE STRUCTURE COMPONENTS

Fractions of bars, lenses and rings are calculated as a function of Hubble type, and are also given in different bulge-to-total (B/T) flux-ratio and in absolute magnitude bins in K band. Tables 1–3 give the values for all galaxies in NIRS0S,[4] whereas in Tables 4–6 the values for the barred galaxies are given. In Tables 1 and 4, the Hubble-type bin $-4 \leq T < -3.5$ is not shown, because these galaxies very seldom have any sub-structures. In the lowest galaxy luminosity bin (Tables 3 and 6) the galaxy numbers are shown, but no percentages are given. The percentages in the tables are calculated with respect to the total number of galaxies in each bin. The fractions in Tables 1–6 were calculated also including only the S0−S0/a galaxies (thus excluding Sa galaxies), but are not shown in the tables, as there were no significant changes. The uncertainties are estimated from $\Delta p = \sqrt{(1 - p)p/N}$, where p denotes the

[4] Including the 29 galaxies not forming part of the magnitude-limited sample.

fraction among N galaxies. In the tables, 'res' means that included in the analysis are the weak structures visible only in the residual or unsharp mask images. In all the following the subtypes r'l or R'L are included in the categories rl and RL, respectively.

The absolute magnitudes were calculated using the extended K-band apparent magnitudes taken from 2MASS (Skrutskie et al. 2006). The distances are from the Catalog of Nearby Galaxies by Tully (1988), which uses $H_0 = 75 \, \text{km s}^{-1} \, \text{Mpc}^{-1}$. A correction for Galactic extinction was made using the values given in NASA Extragalactic Database (NED), based on the maps of Schlegel, Finkbeiner & Davies (1998). As explained in Laurikainen et al. (2010), the B/T values are corrected for Galactic and internal extinction using different corrections for the bulge and the disc (Graham & Worley 2008). By bulge we mean the flux fitted by the Sérsic function, and by the disc all the remaining flux, which includes not only the exponential disc but also the bars, ovals and lenses.

3.1 Bars

The bar fraction (SB+SAB) we find among the S0$^+$ galaxies ($T = -1$) is as high as for spirals ($T = 1$), e.g. ∼80 per cent have bars. It gradually drops towards the earlier type systems, being 50 ± 8 per cent among the S0^o's ($T = -2$), and 35 ± 7 per cent among the S0$^-$ types ($T = -3$) (Table 1). The tendency is the same separately for strong (B) and weak (AB) bars (see Fig. 2a). The tendency of lower bar fractions among the S0 galaxies, compared to spirals, have been previously shown by Laurikainen et al. (2009) using near-IR images for 360 galaxies at $z \sim 0$, and by Nair & Abraham (2010a; using 14 000 optical images) at $z = 0.01$–0.1. The obtained bar fractions among the S0s and spirals were 46 per cent versus ∼65 per cent at

Table 2. Fractions of structure components in B/T bins, for *complete NIRS0S*.

B/T bin: (N_{tot} in bin)	0–0.2 (55)	0.2–0.3 (56)	0.3–0.4 (41)	> 0.4 (53)
Bars:				
A	38 ± 7 (21)	30 ± 6 (17)	37 ± 8 (15)	66 ± 7 (35)
AB	22 ± 6 (12)	39 ± 7 (22)	44 ± 8 (18)	15 ± 5 (8)
B	40 ± 7 (22)	29 ± 6 (16)	17 ± 6 (7)	17 ± 5 (9)
B+AB	64 ± 6 (35)	68 ± 6 (38)	61 ± 8 (25)	32 ± 6 (17)
Lenses:				
L	9 ± (5)	11 ± 4% (6)	22 ± 6% (9)	9 ± 4% (5)
l	7 ± 4 (4)	14 ± 5% (8)	24 ± 7% (10)	26 ± 6% (14)
nl	9 ± 4 (5)	21 ± 5% (12)	20 ± 6% (8)	11 ± 4% (6)
bl	24 ± 6 (13)	29 ± 6% (16)	15 ± 5% (6)	2 ± 2% (1)
L, RL	24 ± 6 (13)	34 ± 6% (19)	34 ± 7% (14)	15 ± 5% (8)
RL	15 ± 5 (8)	23 ± 6% (13)	12 ± 5% (5)	6 ± 3% (3)
l, rl	18 ± (10)	30 ± 6% (17)	41 ± 7% (17)	32 ± 6% (17)
rl	11 ± 4 (6)	16 ± 5% (9) 1	17 ± 6% (7)	6 ± 3% (3)
nl, rnl	11 ± 4 (6)	23 ± 6% (13)	20 ± 6% (8)	17 ± 5% (9)
Rings:				
Outer	16 ± 5 (9)	23 ± 6% (13)	12 ± 5% (5)	6 ± 3% (3)
inner(r, rs)	16 ± 5 (9)	14 ± 5% (8)	7 ± 4% (3)	7 ± 4% (4)
Nuclear	9 ± 4 (5)	9 ± 4% (5)	12 ± 5% (5)	–

Table 3. Fractions of structure components in bins of absolute galaxy magnitudes in K band, for *complete NIRS0S*.

Magnitude bin: (N_{tot} in bin)	−20 to −22 (7)	−22 to −24 (96)	−24 to −26 (102)
Bars:			
A	(2)	26 ± 5% (25)	59 ± 5% (60)
AB	(1)	36 ± 5% (35)	24 ± 4% (24)
B	(4)	35 ± 5% (34)	16 ± 4% (16)
B+AB	(5)	73 ± 5% (70)	39 ± 5% (40)
nb(res)	(–)	26 ± 4% (25)	18 ± 4% (18)
Lenses:			
L	(2)	14 ± 4% (13)	10 ± 3% (10)
l	(–)	16 ± 4% (15)	21 ± 4% (21)
nl	(1)	14 ± 3% (13)	17 ± 4% (17)
bl	(2)	25 ± 4% (24)	10 ± 3% (10)
multi$_l$	(1)	10 ± 3% (9)	8 ± 3% (8)
L, RL	(4)	32 ± 5% (31)	19 ± 4% (19)
l, rl	(–)	31 ± 5% (30)	31 ± 4% (31)
nl, rnl	(1)	18 ± 4% (17)	18 ± 4% (18)
multi$_{l,rl}$	(1)	22 ± 4% (21)	17 ± 4% (17)
Rings:			
Outer	(1)	18 ± 4% (17)	12 ± 3% (12)
Inner(r, rs)	(2)	20 ± 4% (19)	3 ± 2% (3)
Nuclear	(1)	10 ± 3% (10)	4 ± 2% (4)

$z = 0$ and 12 per cent versus 22 per cent at $z = 0.01$–0.1, respectively. In both studies, the classification and the identification of bars were done visually. The large differences in the bar fractions are mainly because Nair and Abraham detected only strong bars, whereas we include also weak bars into the statistics. A fairly low bar fraction among the S0s has been found also by Aguerri, Méndez-Abreu & Corsini (2009) at $z = 0.01$–0.04, the fractions being 29 per cent and 55 per cent for the S0s and spirals, respectively. However, in their study the Hubble type was based on the concentration parameter (see Conselice, Bershady & Jangren 2000). Taking into account the large range of B/T flux-ratio within one Hubble type (see Laurikainen et al. 2010) the bar fractions obtained by Aguerri et al. and Laurikainen et al. are not directly comparable: in Aguerri et al., the implicit association of high B/T for the S0s causes a bias towards the early-type S0s, which have higher B/T flux-ratios and a lower fraction of bars.

The bar fraction depends on the B/T flux-ratio and the luminosity of the galaxy (Tables 2 and 3, respectively). It is clearly higher in fainter galaxies, the fractions being $73 ± 5$ per cent and $39 ± 5$ per cent in the galaxy luminosity bins of $-22 > M_K \geq -24$ and $-24 > M_K \geq -26$, respectively. This is the case also separately for strong (B) and weak (AB) bars, and when only the S0−S0/a galaxies are considered. The fraction of strong bars increases towards a lower B/T flux-ratio (Fig. 2b). The Sérsic index n (Fig. 2c) is also interesting, since the bulges in the strongly barred galaxies are more exponential than those in weakly barred or in non-barred galaxies. Although all the family classes cover a similar wide range of n values, the peak values are shifted with respect to each other: $n_{peak} \sim 1.75$, 2.25 and 2.75 for B, AB and A families, respectively. The Kolmogorov–Smirnov (KS) test shows that the distributions of SA and SB galaxies in Figs 2b and 2c are different ($p = 0.1$ per cent and 3.4 per cent, respectively).

Compared to non-barred galaxies, lower B/T flux-ratios in barred early-type spirals have been previously found by Laurikainen et al. (2007) and Weinzirl et al. (2009). A similar result was obtained also by Coelho & Gadotti (2011) for disc galaxies, without specifying the morphological type. For the S0s somewhat different results have been obtained depending on the exact sample used (Laurikainen et al. 2007, 2010). Based on the results of the current study, this can be understood, because the relative fraction of strong and weak bars varies in these S0 galaxy samples: including a large fraction of weak bars any difference in B/T flux-ratio between barred and non-barred galaxies is easily diluted (like in Laurikainen et al. 2010). Bar fractions in the lower luminosity spirals, e.g. in very late type spirals, have been studied by Barazza, Jogee & Marinova (2008): they found that the galaxies with smaller B/T flux-ratios have a larger fraction of bars. It is worth noting that the bars in the lower luminosity galaxies are not necessarily similar to those in the bright galaxies.

Table 4. Fractions of structure components in different Hubble types in *barred galaxies* in the complete NIRS0S.

Barred Hubble stage: (N_{tot} in bin)	−3 (17)	−2 (20)	−1 (27)	0 (22)	1 (27)
Bars:					
nb	29 ± 11% (5)	35 ± 11% (7)	26 ± 8% (7)	23 ± 9% (5)	11 ± 6% (3)
nb+nb$_{res}$	41 ± 12% (7)	45 ± 11% (9)	48 ± 10% (13)	27 ± 9% (6)	29 ± 9% (8)
B$_a$	12 ± 8% (2)	30 ± 10% (6)	19 ± 7% (5)	–	14 ± 7% (4)
AB$_a$	18 ± 9% (3)	20 ± 9% (4)	19 ± 7% (5)	18 ± 8% (4)	7 ± 5% (2)
B$_{ax}$	11 ± 7% (2)	40 ± 10% (8)	22 ± 8% (6)	9 ± 6% (2)	19 ± 7% (5)
AB$_{ax}$	17 ± 8% (3)	20 ± 9% (4)	26 ± 8% (7)	18 ± 8% (4)	15 ± 7% (4)
BAB$_{ax}$	29 ± 11% (5)	60 ± 11% (12)	48 ± 10% (13)	27 ± 9% (6)	33 ± 9% (9)
multi$_{bar}$	18 ± 9% (3)	20 ± 9% (4)	26 ± 8% (7)	18 ± 8% (4)	11 ± 6% (3)
multi$_{bar}$(res)	29 ± 11% (5)	30 ± 10% (6)	44 ± 10% (12)	23 ± 9% (5)	26 ± 8% (7)
Lenses:					
L	59 ± 12% (10)	25 ± 9% (5)	11 ± 6% (3)	4 ± 4% (1)	4 ± 4% (1)
l	41 ± 12% (7)	20 ± 9% (4)	11 ± 6% (3)	5 ± 4% (1)	11 ± 6% (3)
nl	6 ± 6% (1)	20 ± 9% (4)	22 ± 8% (6)	18 ± 8% (4)	18 ± 7% (5)
bl	18 ± 9% (3)	45 ± 11% (9)	41 ± 9% (11)	32 ± 10% (7)	30 ± 9% (8)
multi$_l$	18 ± 9% (3)	15 ± 8% (3)	7 ± 5% (2)	–	7 ± 5% (2)
L, RL	59 ± 12% (10)	40 ± 11% (8)	37 ± 9% (10)	36 ± 10% (8)	11 ± 6% (3)
RL	–	15 ± 8% (3)	26 ± 8% (7)	32 ± 10% (7)	7 ± 5% (2)
l, rl	41 ± 12% (7)	25 ± 10% (5)	41 ± 9% (11)	23 ± 9% (5)	22 ± 8% (6)
rl	–	5 ± 5% (1)	30 ± 9% (8)	18 ± 8% (4)	11 ± 6% (3)
nl, rnl	12 ± 8% (2)	30 ± 10% (6)	26 ± 8% (7)	23 ± 9% (5)	19 ± 7% (5)
multi$_{l,rl}$	24 ± 10% (4)	30 ± 10% (6)	30 ± 9% (8)	18 ± 8% (4)	11 ± 6% (3)
Rings:					
Outer	–	10 ± 7% (2)	30 ± 9% (8)	23 ± 9% (5)	44 ± 10% (12)
Inner(r, rs)	–	10 ± 7% (2)	33 ± 9% (9)	18 ± 8% (4)	11 ± 6% (3)
Nuclear	–	5 ± 5% (1)	30 ± 9% (8)	9 ± 6% (2)	11 ± 6% (3)

Table 5. Fractions of structure components in B/T bins in *barred galaxies* in the complete NIRS0S.

Barred B/T bin: (N_{tot} in bin)	0–0.2 (35)	0.2–0.3 (37)	0.3–0.4 (25)	> 0.4 (18)
Bars:				
nb	11 ± 5% (4)	22 ± 7% (8)	36 ± 10% (9)	17 ± 9% (3)
nb+nb$_r$	20 ± 7% (7)	38 ± 8% (14)	44 ± 10% (11)	17 ± 9% (3)
B$_a$	20 ± 7% (7)	16 ± 6% (6)	4 ± 4% (1)	17 ± 9% (3)
AB$_a$	9 ± 5% (3)	22 ± 7% (8)	24 ± 9% (6)	6 ± 5% (1)
B$_{ax}$	23 ± 7% (8)	22 ± 7% (8)	8 ± 5% (2)	28 ± 11% (5)
AB$_{ax}$	11 ± 5% (4)	24 ± 7% (9)	24 ± 8% (6)	17 ± 9% (3)
BAB$_{ax}$	34 ± 8% (12)	46 ± 8% (17)	32 ± 9% (8)	44 ± 12% (8)
multi$_{bar}$	20 ± 7% (7)	38 ± 8% (14)	44 ± 10% (11)	17 ± 9% (3)
Lenses:				
L	14 ± 6% (5)	13 ± 6% (5)	32 ± 9% (8)	11 ± 7% (2)
l	3 ± 3% (1)	8 ± 5% (3)	28 ± 9% (7)	33 ± 11% (6)
nl	6 ± 4% (2)	24 ± 7% (9)	28 ± 9% (7)	17 ± 9% (3)
bl	37 ± 8% (13)	43 ± 8% (16)	24 ± 8% (6)	6 ± 5% (1)
multi$_l$	8 ± 5% (3)	8 ± 5% (3)	28 ± 9% (7)	33 ± 11% (6)
L, RL	31 ± 8% (11)	40 ± 8% (15)	48 ± 10% (12)	22 ± 10% (4)
RL	17 ± 6% (6)	27 ± 7% (10)	16 ± 7% (4)	11 ± 7% (2)
l, rl	17 ± 6% (6)	27 ± 7% (10)	48 ± 10% (12)	44 ± 12% (8)
rl	14 ± 6% (5)	19 ± 6% (7)	20 ± 8% (5)	11 ± 7% (2)
nl, rnl	9 ± 5% (3)	27 ± 7% (10)	28 ± 9% (7)	33 ± 11% (6)
multi$_{rl}$	9 ± 5% (3)	24 ± 7% (9)	20 ± 8% (5)	33 ± 11% (6)
multi$_{l,rl}$	17 ± 6% (6)	32 ± 8% (12)	48 ± 19% (12)	50 ± 12% (9)
Rings:				
Outer	23 ± 7% (8)	35 ± 8% (13)	16 ± 7% (4)	11 ± 7% (2)
Inner(r, rs)	17 ± 6% (6)	19 ± 6% (7)	12 ± 6% (3)	11 ± 7% (2)
Nuclear	14 ± 6% (5)	11 ± 5% (4)	20 ± 8% (5)	–

Table 6. Fractions of structure components in bins of absolute galaxy brightness in *K* band, for *barred galaxies* in the complete NIRS0S.

| Barred Magnitude bin: (N_{tot} in bin)		−20 to −22 (5)	−22 to −24 (70)	−24 to −26 (40)
Bars:				
nb	(−)		23 ± 5% (16)	15 ± 6% (6)
nb+nb$_{res}$	(−)		31 ± 5% (22)	33 ± 7% (13)
B$_a$	(1)		14 ± 4% (10)	15 ± 6% (6)
AB$_a$	(0)		19 ± 5% (13)	13 ± 5% (5)
B$_{ax}$	(1)		20 ± 5% (14)	20 ± 6% (8)
AB$_{ax}$	(−)		23 ± 5% (16)	15 ± 6% (6)
BAB$_{ax}$	(1)		43 ± 6% (30)	38 ± 8% (15)
multi$_{bar}$	(−)		31 ± 6 (22)	33 ± 7 (13)
Lenses:				
L	(1)		19 ± 5% (13)	15 ± 6% (6)
l	(0)		17 ± 5% (12)	13 ± 5% (5)
nl	(0)		16 ± 4% (11)	25 ± 7% (10)
bl	(2)		34 ± 6% (24)	25 ± 6% (10)
multi$_l$	(1)		14 ± 5 (10)	20 ± 6 (8)
L, RL	(3)		40 ± 6% (28)	28 ± 7% (11)
RL	(1)		21 ± 5% (15)	12 ± 5% (5)
l, rl	(0)		36 ± 6% (25)	28 ± 7% (11)
rl	(0)		18 ± 5% (13)	15 ± 6% (6)
nl, rnl	(0)		21 ± 5% (15)	28 ± 7% (11)
multi$_{l,rl}$	(1)		10 ± 3 (7)	30 ± 7 (12)
Rings:				
Outer	(1)		23 ± 5% (16)	25 ± 10% (10)
Inner(r, rs)	(2)		20 ± 5% (14)	5 ± 3% (2)
Nuclear	(1)		13 ± 4% (9)	10 ± 5% (4)

3.2 Barlenses

In the NIRS0S Atlas, barlenses were identified as lens-like structures inside the bar and they were suggested to form part of the bar itself. We found that the occurrence of a barlens does not depend on the Hubble type (Fig. 3a) or on the galaxy luminosity. The fractions of barlenses in the two absolute magnitude bins are 34 ± 6 per cent and 25 ± 6 per cent, respectively (Table 6). In Table 7, the fractions of the structure components in barred S0−S0/a galaxies with barlenses are compared with those without a barlens. The clearest difference is that even 52 ± 9 per cent of the barlens galaxies have ansae in the main bars, whereas among the galaxies without any barlens only 24 ± 6 per cent of bars have ansae. Another noticeable characteristic is that in the barlens galaxies multiple lenses are rare: only 24 ± 8 per cent of them have multiple lenses, compared to 56 ± 7 per cent in barred galaxies without a barlens. The occurrence of a barlens is strongly connected to the properties of the bulges so that their fraction increases towards the lower *B/T* flux-ratios (Fig. 3b) and lower values of the Sérsic index (Fig. 3c). These characteristics are partly related to the fact that barlenses are more common among the strongly barred galaxies (62 ± 9 per cent and 38 ± 9 per cent among the B and AB families, respectively; see Table 9), which also have fairly low *B/T* flux-ratios and small values of the Sérsic index.
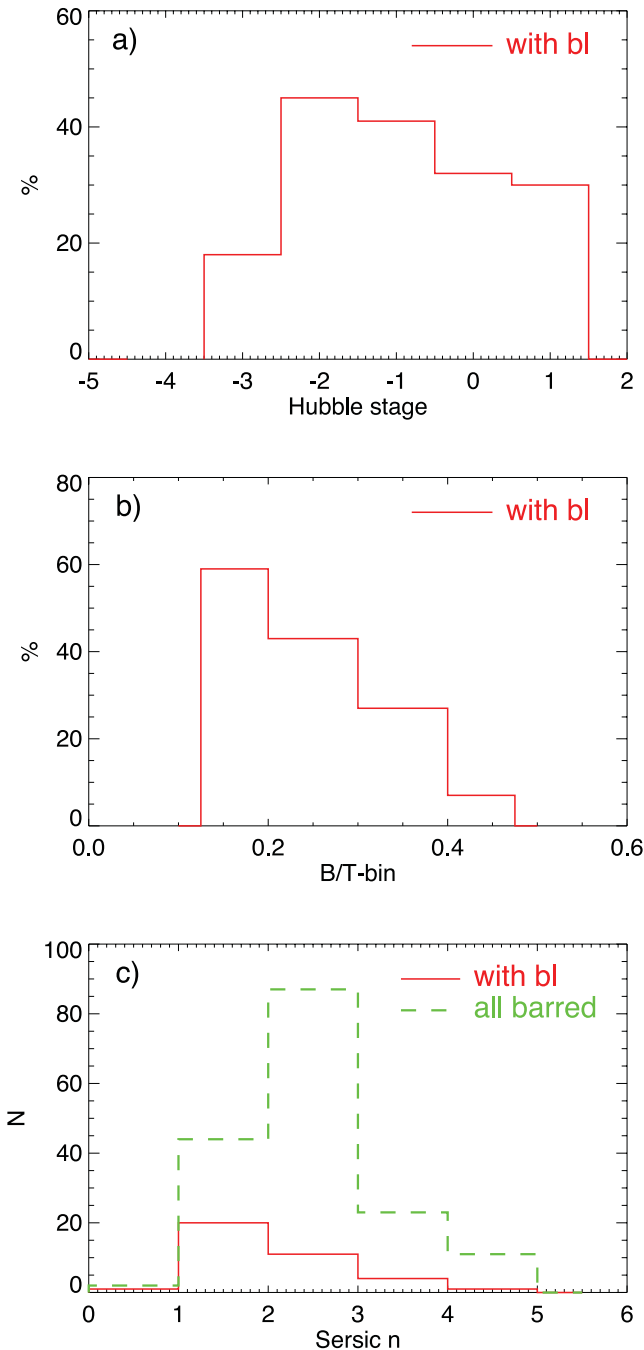
3.3 Rings, ringlenses and lenses

3.3.1 Frequency as a function of Hubble type

Lenses are common features in the early-type disc galaxies (see also Laurikainen et al. 2005, 2009, 2011; Nair & Abraham 2010b), and are crucial for identifying the S0s. Lenses are found to be distributed
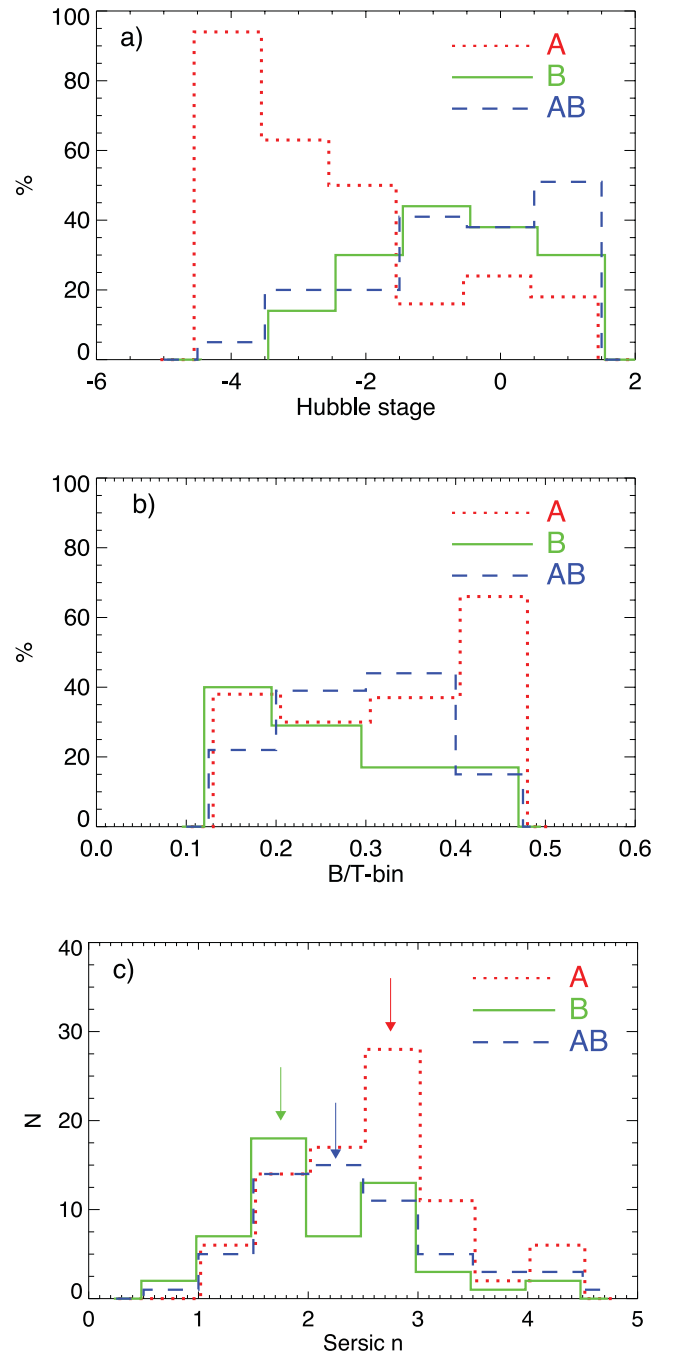
Figure 2. Galaxy fractions of different family classes (A, AB, B) are shown as a function of Hubble type (a), bulge-to-total (*B/T*) flux-ratio (b) and the value of the Sérsic index *n* (c). The statistics is based on the complete NIRS0S (include S0−Sa types). The fractions given in percentages are calculated with respect to the galaxy number in each *B/T* or Hubble-type bin. The same is done in all following similar figures.

over all Hubble types in NIRS0S, but the fully developed lenses (L, l) are more frequent among the early-type S0s ($T = −3$). For barred galaxies this is shown in Fig. 4a (Table 4): among the Hubble-type $T = −3$, even 59 ± 12 per cent of the barred S0s have an outer lens and 41 ± 12 per cent have an inner lens. On the other hand, the fraction of nuclear lenses (∼25 per cent) is nearly constant as a function of Hubble type, until it drops at $T = −3$.

Figure 3. Fractions of barred galaxies with barlenses are shown as a function of Hubble type (a), and B/T flux-ratio (b). In (c) the distribution of the Sérsic index n is shown for the galaxies with barlenses, compared with that for all barred galaxies in NIRS0S.

Table 7. Fractions of structure components among the barred (B+AB) S0+S0/a galaxies: compared are galaxies with (left-hand column) and without barlenses (right-hand column). The x-shaped bars are included into barlenses and the eight nuclear bars without any main bars do not form part of the statistics.

Barred S0−S0/a:		
	have bl	no bl
(N_{tot} in bin)	(28)	(57)
ansae	$52 \pm 9\%$ (15)	$24 \pm 6\%$ (14)
nb	$45 \pm 9\%$ (13)	$38 \pm 6\%$ (22)
nl	$21 \pm 8\%$ (6)	$16 \pm 5\%$ (9)
nl+nrl	$24 \pm 8\%$ (7)	$37 \pm 6\%$ (21)
multi$_{l,rl}$	$24 \pm 8\%$ (7)	$56 \pm 7\%$ (32)

galaxies (Table 8). Using optical images the ring fractions might be even higher because many rings are known to be active star-forming regions (see Buta and Combes 1996; Comerón et al. 2010; Grouchy et al. 2010). It is worth noting that although nuclear lenses appear in all Hubble types, nuclear rings are more concentrated in late-type S0s ($T = -1$), in a similar manner as inner rings.

3.3.2 The parent galaxy properties

As rings and ringlenses are assumed to be related phenomena, also their parent galaxy properties are expected to be similar. Indeed, we find that the distributions of the B/T flux-ratios are similar (Fig. 4e,f). However, the galaxies with full lenses have higher B/T flux-ratios, being typically larger than 0.3 (Fig. 4d). Again, the tendencies are similar among the inner and outer rings and among the inner and outer ringlenses. In the highest B/T bin there are more inner (l) than outer lenses (L), which might be partly because the shallow outer lenses are more difficult to detect.

The appearance of rings, ringlenses and lenses is not very sensitive to galaxy luminosity. However, while lumping together the outer lenses (L) and ringlenses (RL) they appear more frequently among the fainter galaxies (32 ± 5 per cent versus 19 ± 4 per cent in the two galaxy luminosity bins, respectively; Table 3). Also, the inner rings (r,rs) appear more frequently among the fainter galaxies (20 ± 4 per cent versus 3 ± 2 per cent, in the two bins, respectively). The tendencies are similar if only the barred galaxies are considered (Table 6).
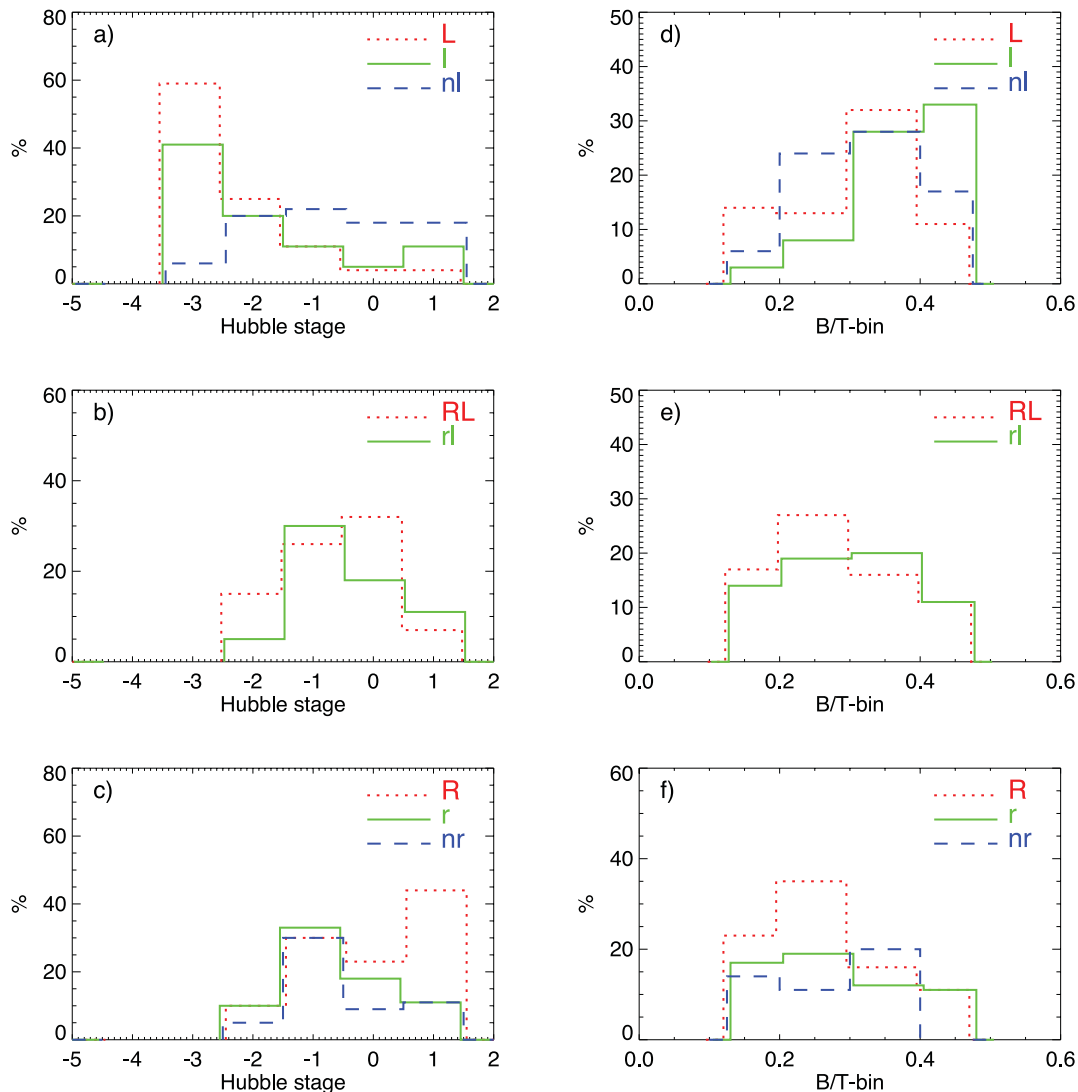
In conclusion, rings and ringlenses are common in the early-type spirals and in the late-type S0s, whereas the fully developed lenses are more common in the early-type S0s. There is no strong dependence of the type of structure on galaxy luminosity. However, the galaxies with full lenses typically have higher B/T flux-ratios than the galaxies with rings or ringlenses. On the other hand, the occurrence of nuclear lenses does not depend on the Hubble type or on the properties of the bulge.

3.4 Multicomponent structures

3.4.1 Multiple bars

Multiple bars have been previously detected in ~30 per cent of the barred galaxies and in ~20 per cent of all early-type disc galaxies, by Erwin & Sparke (2002) and by Laine et al. (2002). The sample of Erwin and Sparke consists of 30 barred S0−S0/a galaxies, of which 10 have double bars. In order to detect also the weak bars they used colour images and applied the unsharp mask techniques. The

A significant fraction of the inner rings and ringlenses appear at Hubble-type $T = -1$, after which the fraction gradually drops towards the later types (Fig. 4b,c). Outer rings also appear in the S0s, but they are even more common in the early-type spirals. Rings are generally thought to be resonance structures of bars (Athanassoula & Bosma 1985; Buta 1995) or linked to resonances via bar-driven manifolds (Athanassoula et al. 2010). They indeed appear mainly in barred galaxies, the fractions of outer, inner and nuclear rings being 14 per cent, 17 per cent and 12 per cent, respectively, in contrast to the ring fractions of 1–7 per cent among the non-barred

Figure 4. Fractions of the different structure components in barred galaxies are shown, as a function of Hubble type (a)–(c) and as a function of *B/T* flux-ratio (d)–(f). The identifications of the structures are from NIRS0S Atlas (the types rl and RL include also their subtypes r'l and R'L).

Table 8. Fractions of inner, outer and nuclear rings among the barred and non-barred galaxies. The barred galaxies include both strong (B) and weak (AB) bars (uses *complete NIRS0S*, e.g. S0–Sa types).

Fraction of (N_{tot} in bin)	In barred (115)	In non-barred (79)
Inner ring	$17 \pm 3\%$ (20)	$7 \pm 3\%$ (6)
Outer ring	$14 \pm 3\%$ (16)	$4 \pm 2\%$ (3)
Nuclear ring	$12 \pm 3\%$ (14)	$1 \pm 1\%$ (1)

double-bar catalogue by Erwin (2004) is larger, including 38 multiple barred S0+S0/a galaxies collected from the literature. However, as noticed by Erwin the catalogue is most probably biased towards peculiar and strongly barred galaxies, since it is randomly collected from different sources. These results are discussed also in the recent review by Erwin (2011). The fractions of double bars in the early-type disc galaxies have been studied also by Laurikainen et al. (2009) for a sub-sample of 127 galaxies in NIRS0S largely confirming the previous results.

Among the S0–S0/a galaxies, we detect 35 multiple bars, which makes 20 ± 3 per cent of all, and 30 ± 5 per cent of the barred S0+S0/a galaxies, fully confirming the previous results. However, it is worth noting that compared to Erwin & Sparke (2002), the total number of double bars in NIRS0S is approximately three times larger. The NIRS0S double-bar sample is comparable in size with that of the double-bar catalogue by Erwin (2004), but has the advantage of being magnitude-limited and therefore more complete in a statistical sense. Both in this study and in Erwin & Sparke (2002) unsharp masks were used to identify the faint nuclear bars. Alternatively, we also applied a decomposition approach for detecting the weak bars in the residual images, after subtracting the bulge model from the original image. These methods of detecting multiple bars are important, because even 40 per cent of all nuclear bars are weak or overshadowed by massive bulges in the direct images. Erwin & Sparke (2002) also showed that the fractions of double bars are similar in S0, S0/a and Sa galaxies, which we confirm. We further show that there are no systematic differences in the multiple-bar fractions between the different subtypes of the S0s (Fig. 5a). In Figs 5b and 5c, we also show that the occurrence of a nuclear bar is not strongly connected to the properties of the bulges: they appear
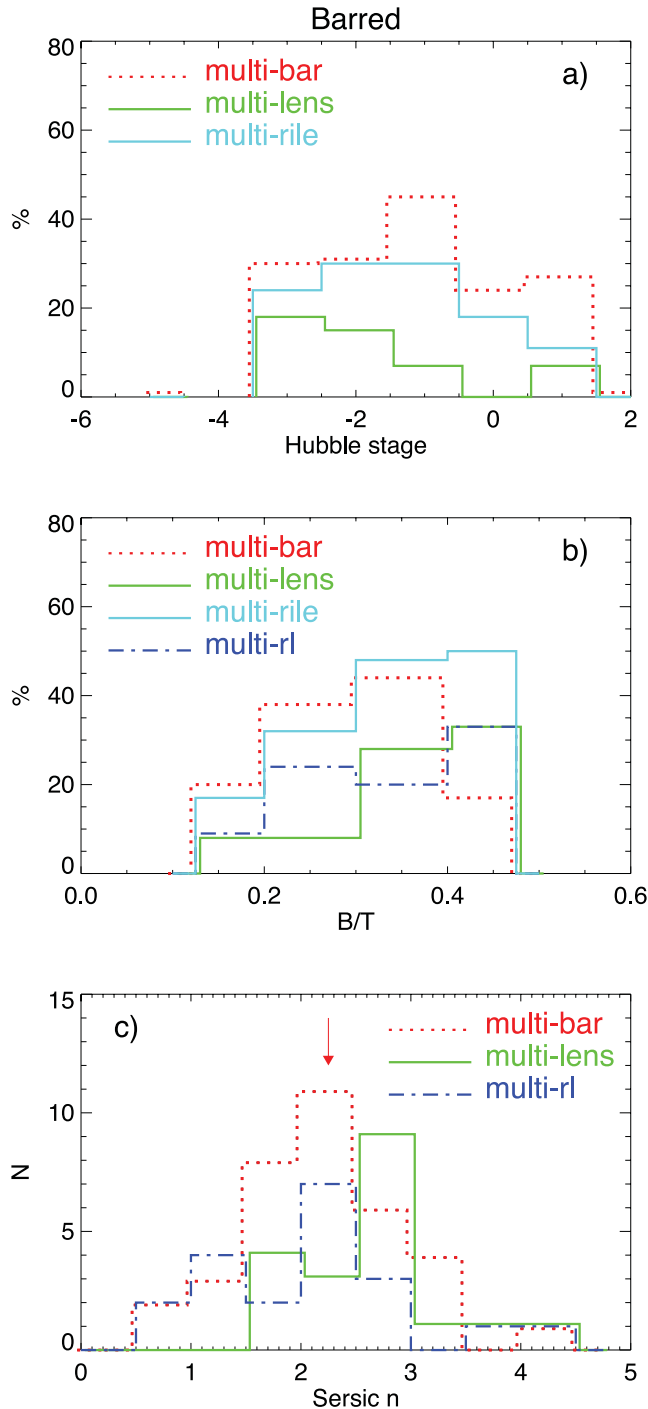
Figure 5. Fractions of multiple components in barred galaxies: (a) as a function of Hubble type, (b) B/T flux-ratio (c) and the values of Sérsic index. In the panels *multi-bar* = multiple bars, *multi-lens* = multiple lenses in which both lenses are fully developed (l,L), *mult-rl* = multiple ringlenses (rl, RL), *multi-rile* = multiple lenses in which one of the lenses is a ringlens (l, L, rl, RL).

in the whole range of B/T flux-ratios. The Sérsic index is peaked at $n \sim 2.25$.

We also detect seven nuclear bars in galaxies without any main bar, e.g. the bars have similar sizes as typical nuclear bars in barred galaxies. In Table 10, the Hubble types, the bins of the B/T flux-ratios and the galaxy luminosity bins for these galaxies are shown.

It is worth noting that 5/7 of them have very early Hubble types and appear in the bin of the more luminous galaxies in our sample.

3.4.2 Multiple lenses

Multiple lenses have been identified in the early-type disc galaxies a long time ago (Sandage 1961) and have also been discussed in detail for some individual galaxies by Kormendy (1979). One of the most spectacular cases is NGC 1411, which has a series of lenses (Laurikainen et al. 2006; Buta et al. 2007). In Fig. 5, the fractions of multiple lenses are shown, as a function of Hubble type and as a function of the properties of the bulges. Barlenses are excluded here, because they are assumed to form a part of the bar. The following cases are shown: (1) multiple lens systems consisting of only fully developed lenses ('multi-lens'), (2) systems in which one of the lenses has some ring-like characteristics ('multi-rile') and (3) cases in which both lenses have ring-like characteristics ('multi-rl').

We find that although multiple bars appear in all Hubble types in a similar manner, the fully developed multiple lenses are more frequent among the early-type S0s ($T = -3, -2$). However, including also ringlenses, they are more uniformly distributed among all Hubble types. Also, while multiple bars cover a large variety of B/T flux-ratios, multiple lenses are more common in galaxies with $B/T > 0.3$. Furthermore, the Sérsic index in multiple-lens galaxies is peaked at larger values, $n \sim 2.75$, as compared to $n \sim 2.25$ for the galaxies with multiple bars. For the barred galaxies this is shown in Fig. 5 (Tables 4 and 5).

In the NIRS0S Atlas, multiple lenses were found in 25 ± 3 per cent of the S0−S0/a galaxies (the above categories 1 and 2 combined). Focusing only on fully developed lenses (category 1) the fraction is reduced to 11 ± 3 per cent. Even 61 per cent of all multiple lenses (all three categories combined) appear in barred galaxies. Of the fully developed lenses the fraction is somewhat lower, 42 per cent of them being barred.

3.5 Structures in the A, AB and B families

An important new result of this study is that nuclear bars appear preferentially in galaxies with weak main bars. Namely, we found that even 44 ± 8 per cent of the galaxies with weak bars (AB), and only 24 ± 6 per cent with strong (B) bars have nuclear bars (Table 9). These numbers include the faint nuclear bars detected only in the residual images. Notice that Erwin & Sparke (2002) found equal nuclear bar fractions among the strongly and weakly barred systems. Possible reasons for this difference, compared to our result, are that the sample by Erwin and Sparke is smaller (10 double-barred galaxies) and might be biased towards peculiar strongly barred galaxies that have a smaller number of multiple bars. Also, for one-half of the galaxies optical images were used in their study and therefore some of the weak nuclear bars might have also been hidden by dust. Most probably the larger sample by Erwin (2004) is missing galaxies with weak main bars and therefore is not suitable to study the effect.

The barlens is an other structure component for which the frequencies are different among the strongly and weakly barred galaxies: the fractions are 62 ± 9 per cent versus 38 ± 9 per cent among the B and AB families, respectively. The differences in the fractions of all the other structures components between the B and AB families are only marginal. It is also interesting that although the fractions of the structure components in the non-barred galaxies (A) are typically very small (3–10 per cent), even 21 per cent of them

Table 9. Fractions of structure components in A, AB and B family classes for the complete NIRS0S. For the S0−S0/a galaxies calculated are also the fractions of nuclear bars among the strongly (B) and weakly (AB) barred galaxies, as well as the fractions of barlenses in the same family classes. In parentheses the total numbers of galaxies in the different family classes are given.

Family	A	AB	B
complete NIRS0S:			
(N_{tot} in bin)	(82)	(57)	(52)
L	5 ± 2% (4)	16 ± 5% (9)	19 ± 4% (12)
l	21 ± 4% (17)	21 ± 5% (12)	16 ± 4% (6)
nl	10 ± 3% (8)	23 ± 6% (13)	20 ± 4% (9)
RL	6 ± 3% (5)	23 ± 6% (13)	21 ± 4% (10)
rl	9 ± 3% (7)	23 ± 6% (13)	17 ± 4% (6)
nrl	– (0)	4 ± 2% (2)	5 ± 2% (3)
R	4 ± 2% (3)	30 ± 6% (17)	25 ± 4% (10)
r	6 ± 3% (5)	12 ± 4% (7)	17 ± 4% (12)
nr	– (0)	16 ± 5% (9)	14 ± 3% (6)
S0+S0/a:			
(N_{tot} in bin)	(54)	(41)	(42)
bl	–	38 ± 9% (11)	62 ± 9% (18)
no bl	–	54 ± 6% (31)	45 ± 6% (26)
nb	13 ± 5% (7)	44 ± 8% (18)	24 ± 6% (19)

Table 10. Nuclear bars in the non-barred galaxies. The numbers are given in bins of the Hubble-type T, B/T and in the three magnitude bins. The bins are: bin1 $= -22 \leq M_K < -20$, bin2 $= -24 \leq M_K < -22$, bin3 $= -26 \leq M_K < -24$.

T range:	−3 (2), −2 (2), −1 (1), 0 (1), 1 (1)
Mag range:	bin1 (0), bin2 (2), bin3 (5)
B/T range	0–0.2 (0), 0.2–0.3 (1), 0.3–0.4 (2), >0.4 (4)

have inner lenses (l). In fact, the fraction of the inner lenses is found to be constant among all the family classes (see Table 9).

4 DIMENSIONS OF THE STRUCTURES

The dimensions of the structure components are studied using the measurements given in the NIRS0S Atlas (Tables 5 and 6), after converting them to the plane of the galactic disc. No internal extinction corrections were applied to the lengths. In the Atlas, two additional length estimations are provided for many of the bars, based on the radial profiles of the ellipticities, but as only the visual length estimation is available for all bars, it is used in this study.

4.1 Bars

The main bars were found to have a mean size (= semi-major axis length) of ~4 kpc, in agreement with the previous studies (see for example Erwin 2005, 2011). No difference was found in the main bar sizes between single and multiple bar galaxies, the mean sizes being 4.1 ± 0.4 kpc and 4.4 ± 0.4 kpc, respectively (see Table 11). This differs from Erwin (2011) who found smaller bars in galaxies with single bars, with typical sizes of ~2.5 kpc. A possible reason for this discrepancy is that some single bars in the NIRS0S Atlas were classified as nuclear bars, based on their small sizes in respect of the galaxy diameter. Some of such small bars in the sample by Erwin might have been considered as main bars.

The sizes of nuclear bars in our sample cover the range of 0.1–1.5 kpc (with the mean of 0.7 ± 0.4 kpc), comparable with that obtained by Erwin (2005, 2011) who gave a size range of 0.1–1.2 kpc. Nuclear bars in galaxies that do not have any main bar, have the sizes of 0.3–0.9 kpc, well within the range of typical sizes of nuclear bars.
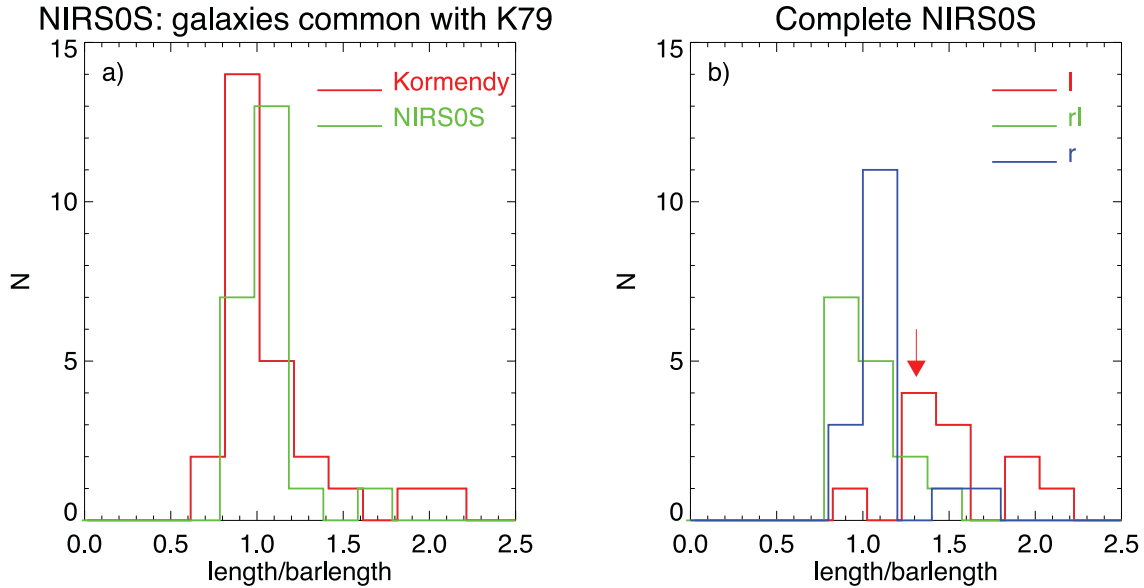
4.2 Rings and lenses, normalized to bar length

4.2.1 Comparison to Kormendy (1979)

The dimensions of the inner rings (r), lenses (l) and ringlenses (rl) have been previously studied by Kormendy (1979) for a sample of 120 disc systems, including 41 S0−S0/a galaxies. These early-type systems form part of the NIRS0S Atlas, thus allowing us to compare our measurements with those obtained by Kormendy. In both studies, the lengths were measured in a similar manner. In cases where the assigned Hubble type differed between the two studies, we adopted the one given in NIRS0S Atlas (the classification by Kormendy was based on the second reference catalogue (RC2) of bright galaxies by de Vaucouleurs, de Vaucouleurs & Corwin 1976). Kormendy (1979) normalized the sizes of the structures to the bar size, without deprojecting the images to the disc plane, and the major or minor axis length of the ring/lens was chosen depending on which one was closer to the bar size. This guaranteed that the relative lens/bar size was correctly estimated regardless of the viewing angle.

The comparison to Kormendy (1979) is shown in Fig. 6a, where the length of the structure is normalized to the bar size. It appears that in the overlapping sub-sample of NIRS0S, the lengths of the rings, lenses and ringlenses are very similar in the two studies. The peak values are *length*(r, rl, l)/*length*(bar) ~1 for all structures, e.g. they typically all end up to the bar radius. This similarity in the lengths of bars and inner lenses was used by Kormendy (1979) to suggest that lenses are formed from bars, e.g. there is a process which makes some bars to evolve rapidly into a nearly axisymmetric state. Kormendy excluded three outliers, NGC 936, NGC 4262 and NGC 3412, having *length*/*length*(bar) > 1.3. For the first two galaxies, the lens was considered to be an outer lens by him and for NGC 3412 his bar length measurement was uncertain. In our

Table 11. *Galaxies with multiple lenses and multiple bars*. The mean ratios of the major axis radii (length) of inner and outer lenses are given. In parenthesis are indicated whether only fully developed lenses (l, L) form part of the multiple lens or are ringlenses (rl, RL) also included. The last two values are obtained as peak values in the histograms of the size distributions of the structures, normalized to the bar size. The uncertainties are the standard deviations of the mean.

Multiple lenses:

length(L, RL)/length(l, rl)	1.9 ± 0.2 ($N = 8$)	Barred
length(L, RL)/length(l, rl)	2.5 ± 0.2 ($N = 8$)	Non-barred
length(L)/length(l)	2.85 ± 0.19 ($N = 4$)	All
length(L, RL)/length(l, rl)	1.96 ± 0.14 ($N = 11$)	All
length(L, RL)/length(bl)	3.8	Barred
length(outer ring) = length(inner ring)	2.0	Barred

Multiple bars:

|		
length(bar)/length(nb)	8.0 ± 1.0 ($N = 23$)	Weak (AB) bars
length(bar)/length(nb)	6.1 ± 0.8 ($N = 12$)	Strong (B) bars
length(bar)	4.1 ± 0.4 kpc ($N = 62$)	Non-multibar galaxies
length(bar)	4.4 ± 0.4 kpc ($N = 31$)	Multibar galaxies
length(nb)	0.7 ± 0.3 kpc ($N = 43$)	All nb
length(nb)	0.6 ± 0.2 kpc ($N = 8$)	Without main bar

Figure 6. (a) The lengths of the inner components (rings + ringlenses + lenses), normalized to bar length: 41 galaxies common in NIRS0S and in the sample by Kormendy (1979) are compared. (b) The complete NIRS0S is used, showing the lengths separately for the rings (r), ringlenses (rl) and lenses (l) (see the details in Section 4.2). The arrow indicates the peak value for the lens distribution.

measurements there is one outlier, NGC 4612, but in this galaxy the lens is truly larger than the bar. As this galaxy has also an outer ringlens, the structure we assign as an inner lens cannot be a misclassified outer lens. However, it is worth noting that although our length measurements are in good agreement with those of Kormendy (1979) the structures classified as lenses (l) by Kormendy (67 ± 9 per cent are lenses) are largely ringlenses (rl) or rings (r) in our classification (only 18 ± 8 per cent are lenses). It seems that we have interpreted the broad dispersed rings as real rings or ringlenses, whereas Kormendy has interpreted them as lenses. In total, the sample by Kormendy has only a few galaxies having structures that we call as lenses. In his study, Kormendy used red and blue Palomar Sky Survey copy plates.

4.2.2 Using complete NIRS0S sample

Next we look at the normalized sizes of the structures in the complete NIRS0S. The following peak values were found: *length*(r, rl, l)/*length*(bar) = 0.9, 1.1 and 1.3 for rl, r and l, respectively (see Fig. 6b; our bins are 0.2 units wide), indicating that in fact only the rings and ringlenses end at the bar radius, whereas the fully developed lenses are clearly larger than the bar. Using the KS test the difference for the lenses and rings is found to be statistically significant: the probability that their distributions are drawn from the same population is only $p = 0.07$ per cent. For the distributions of ringlenses and lenses the difference is not statistically significant ($p = 4.4$ per cent), nor for the distributions of rings and ringlenses ($p = 86$ per
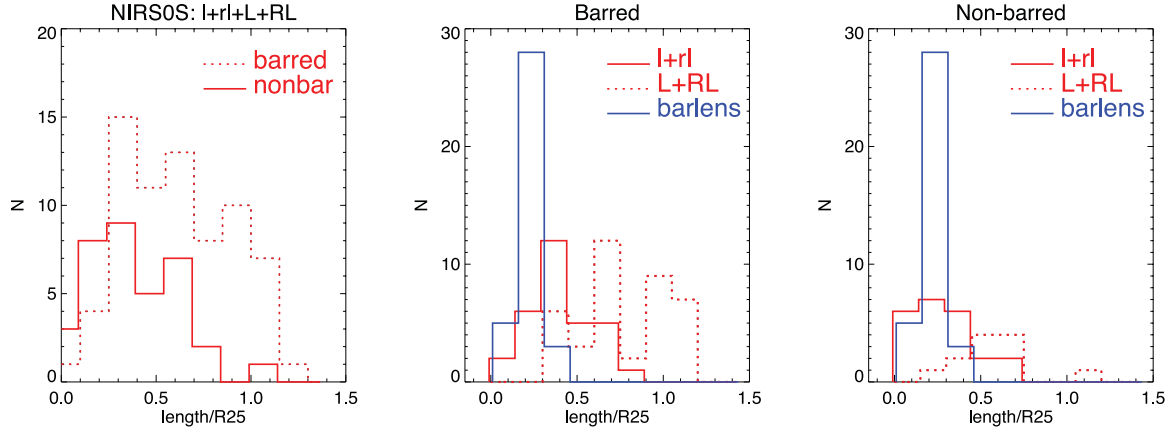
Figure 7. The lengths of the lenses (including ringlenses) in barred and non-barred galaxies in NIRS0S are compared. The sizes are normalized to the galaxy size, R_{25}, given by the radius at the surface brightness of 25 mag arcsec^{-2} in the *B* band, taken from RC3. (a) The sizes of lenses in the barred and non-barred galaxies are shown, including both the inner and outer lenses. In the two other panels, the inner lenses are shown separately for barred (b) and non-barred (c) galaxies. In these panels, the length distribution for the barlenses is also shown: to facilitate comparison with inner lenses in non-barred galaxies, it is shown also in (c).

cent). Although the size difference between the rings and lenses might be partly due to the different ways of measuring the structures (edge of the structure for bars and lenses and the ridge line for rings and ringlenses), it does not wash out the conclusion that the lenses are on average slightly larger than the bar. All structures have also small tails towards larger normalized lengths. Some galaxies were eliminated in the figure for the following reasons: (a) the bar is subtle, peculiar or has an unfavourable orientation in the sky (NGC 1537, NGC 4203, NGC 3489, NGC 6012 and NGC 6438), (b) the dimension of the lens is uncertain (NGC 1371) and (c) the lens most probably is an outer lens (NGC 1389). A particularly high value of $length(\mathrm{l})/length(\mathrm{bar}) = 1.9$ was measured for NGC 5750, but in this galaxy the lens is truly larger than the bar. The galaxy IC 5328, which in the NIRS0S Atlas was interpreted to have a lens [$length(\mathrm{l})/length(\mathrm{bar}) = 0.35$], was excluded because the small lens is in fact a barlens. One can ask whether the fairly large inner lenses [$length(\mathrm{l})/length(\mathrm{bar}){\sim}1.3$–1.5] are actually outer lenses. The answer is that most probably not, because proper outer lenses typically have dimensions of the outer rings or are even larger.

For the outer rings, the normalized lengths peak at $length(\mathrm{R})/length(\mathrm{bar}) = 2.2$, which is in good agreement with the mean value of 2.21 ± 0.12, obtained by Kormendy (1979) and Buta (1995) in the *B* band. For the outer ringlenses (RL) and outer lenses (L) the variations in the lengths are large, the distributions lacking any clear peaks. In those non-barred galaxies, in which a series of lenses are detected, the terminology of inner and outer lenses is merely academic.

4.3 Rings and lenses normalized to galaxy size

In order to compare the dimensions of rings and lenses in barred and non-barred galaxies, the lengths were normalized to the galaxy size, R_{25}. This is the galaxy radius at the surface brightness of 25 mag arcsec^{-2} in the *B* band, taken from the third reference catalogue (RC3) of bright galaxies (de Vaucouleurs et al. 1991). In barred galaxies the bar defines the lens type: the inner lens is located at or near to the bar radius, whereas the outer lens has typically twice the size of the bar, in a similar manner as the inner and outer rings (Kormendy 1979; Buta 1995; Laurikainen et al. 2011). However, in the non-barred galaxies the smaller lens is simply called the inner

lens and the larger one is the outer lens. If only one lens is present, its size relative to the galaxy size defines the inner/outer characteristic. An alternative would be to use some limit in kiloparsecs, based on a typical bar size in galaxies. However, taking into account that the relative bar size varies a lot from one galaxy to another, this is not necessarily a better approach.

The number histograms of the lens dimensions in the barred and non-barred galaxies are compared in Fig. 7 where, for better statistics, lenses and ringlenses are grouped together. The comparison is made first by lumping together the inner and outer structures, which shows that the lenses in the non-barred galaxies are in general clearly smaller (Fig. 7a). This might be partly because more outer lenses are detected in barred galaxies, but that does not explain all of the size differences. This becomes clear when comparing the inner structures (for which better statistics is available) separately for barred and non-barred galaxies (Figs 7b and c): while the peak value for the non-barred galaxies is 0.2, for barred galaxies it is 0.4 (the mean values are 0.28 ± 0.03 and 0.41 ± 0.03, respectively).

The blue histogram in Fig. 7b shows the distribution of barlenses in barred galaxies (for comparison the same histogram is overplotted on Fig. 7c for non-barred galaxies). By definition, $r_{\mathrm{barlens}} \ll r_\mathrm{l}$ is expected. The interesting thing is that the length distribution of the inner lenses in the *non-barred galaxies* (Fig. 7c) is very similar to that for barlenses in *barred galaxies* (the mean value is 0.20 ± 0.01). This is a puzzle that needs to be explained.

4.4 Relative dimensions of lenses in multiple systems

In the following, the relative dimensions of lenses in multiple systems are compared in barred and non-barred galaxies. We are particularly interested in the inner and outer lenses, excluding the nuclear lenses, which leads to the total number of 17 galaxies. This number includes the cases in which the multiple systems are a combination of full (l,L) and intermediate-type (rl, RL) lenses. There is a tendency showing that the mean ratio of the outer to inner lenses is larger for the non-barred galaxies, e.g. $\langle length(\mathrm{L, RL})/length(\mathrm{l, rl}) \rangle = 2.5 \pm 0.2$ ($N = 8$), as compared to 1.9 ± 0.2 ($N = 8$) for the barred galaxies (see Table 11). We can also look at the length ratio separately for those multi-lens systems in which both lenses are fully developed and which gives $\langle length(\mathrm{L})/length(\mathrm{l}) \rangle = 2.85 \pm$

0.19 ($N = 4$). Taking into account the small number statistics the dispersions (what is given is the standard deviation of the mean, equal to STD/$\sqrt{N}$) are fairly small. For NGC 1574, the length ratio is ~5. This galaxy was excluded because the dimension of the outer lens was hard to define accurately.

The average length ratio 1.9 obtained for multiple lenses in barred galaxies is similar to that obtained by us for the outer to inner rings, e.g. *length*(R)/*length*(r) ~ 2.0 (calculated from the peak values of the length distributions for the inner and outer rings, both normalized to bar length). This value is in good agreement with the previous measurements by Kormendy (1979), Athanassoula et al. (1982) and Buta (1995) for the rings.

5 GALAXY LUMINOSITIES AND THE SIZES OF THE STRUCTURES

5.1 Galaxy-luminosity distributions for barred and non-barred galaxies

Distributions of the galaxy luminosities for the barred and non-barred galaxies in the *K* band are shown in Fig. 8. Clearly, there is no upper limit in galaxy luminosity (mass) for bar formation. In Méndez-Abreu et al. (2010) such a cutoff limit was reported to appear at $M_r = -22$ mag, corresponding to $M_K = -25$ mag. Also, barred and non-barred galaxies cover nearly the same range of total galaxy luminosities. However, there is a tendency of increasing mean galaxy luminosity from strongly barred (B) towards weakly barred (AB) and non-barred (A) galaxies. The mean absolute magnitudes in the *K* band are (the uncertainties are standard deviations of the mean)

$\langle M_K \rangle$ (A) $= -24.11 \pm 0.15$,

$\langle M_K \rangle$ (AB) $= -23.78 \pm 0.12$,

$\langle M_K \rangle$ (B) $= -23.52 \pm 0.14$.

It thus appears that the non-barred galaxies are on average 0.6 mag brighter than the strongly barred systems. For the NIRS0S Atlas, the luminosity difference between the barred and non-barred galaxies was indicated also by van den Bergh (2012). The difference in the mean galaxy luminosities between the barred (B+AB) and non-

barred (A) S0s was shown also by Barway, Wadadekar & Kembhavi (2011).

As for the main bars, for the nuclear bars there is no cutoff magnitude limit for the bar formation (Fig. 8). Also, the galaxy luminosity distributions are similar for the barred galaxies in general and separately for the galaxies with nuclear bars.

5.2 Galaxy luminosities and sizes of the structure components

It has been suggested by Kormendy (1979) that galaxy mass uniquely determines the bar size and also the sizes of all the other components associated with the bar, e.g. the inner and outer lenses and the inner and outer rings. He tested this idea showing a correlation between the *B*-band galaxy brightness and the length of the structure. The correlations for all the structure components were found to be tight within one Hubble-type bin. Later type galaxies were systematically shifted towards larger galaxy brightnesses, which were interpreted to follow from their discs having a larger amount of recent star formation. In this study, we can re-investigate this issue in the near-IR, which is much less affected by star formation. We also extend the study to non-barred galaxies and to different subtypes of the S0s.
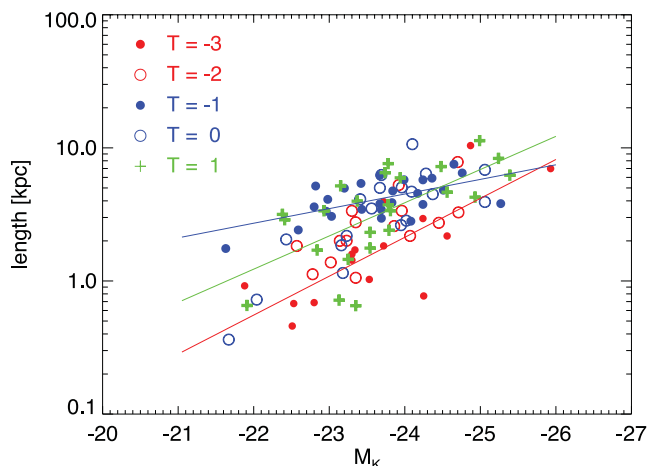
5.2.1 Bars

We confirm the previous result of Kormendy (1979) in a sense that a clear correlation exists between the absolute galaxy magnitude and the length of the bar (Fig. 9). Overall the S0s occupy roughly the same region as the early-type spirals ($T = 1$). However, for a given bar length, the early-type S0s ($T = -3, -2$) are brighter than the late-type S0s ($T = -1$), opposite to the trend found by Kormendy in the optical region. For spirals and for S0 galaxy subtypes the following relations are found:

$T = 1: \quad M_K = -4.0 \log D - 21.6$,

$T = -1: \quad M_K = -9.1 \log D - 18.0$,

$T = -3: \quad M_K = -3.4 \log D - 22.9$,

where *D* stands for bar length in kpc. Combining $T = -3, -2$ the coefficients of correlation are -3.6 and -22.5 and for $T = -1, 0$ they are -4.6 and -21.6. For each morphological type the slope

Figure 8. The number histograms for the barred and the non-barred galaxies, as well as for the nuclear bars, as a function of the absolute galaxy brightness in the *K* band. As explained in the text (Section 3) 2MASS extended apparent magnitudes in the *K* band were used, corrected for Galactic extinction. The distances are from the catalogue by Tully (1988), using the Hubble constant of $H_0 = 75 \text{ km s}^{-1} \text{ Mpc}^{-1}$.

Figure 9. The lengths of bars, inner rings, ringlenses and rings are shown as function of galaxy brightness. The lengths are given in kiloparsecs. The lines are the least-squares fit to the data points in the sub-categories $T = -3$ (red), $T = -1$ (blue) and $T = 1$ (green).

is different from that obtained by Holmberg (1975) between the galaxy luminosity and its diameter, implying that the surface brightness of the bar is not constant. Compared to the Holmberg relation ($dN/d\log D = -5$), the correlation is shallower for $T = -1$ and steeper for $T = -3$. It is worth noting that although the correlation for $T = -1$ is tight, it does not fall between the regression line of the earlier and later Hubble types. This might be related to the fact that the bar length (normalized to galaxy size) maximum appears at $T = -1$ (see fig. 5 in Laurikainen et al. 2007), e.g. all bars in these Hubble types are long, independent of the galaxy luminosity. But still, the physical meaning of this behaviour is unclear.

5.2.2 *Rings and lenses*

As for bars, also for the inner rings, ringlenses and lenses correlations exist between the size of the structure and the galaxy luminosity. The dispersions are large, but they are reduced while plotting the different Hubble types separately (Fig. 10a). There is no obvious difference in the behaviour of rings (r), ringlenses (rl) and lenses (l) (Fig. 10b). However, while comparing the sizes among the barred and non-barred galaxies (Fig. 10c) it appears that the inner structures are smaller for the brightest non-barred galaxies. Similar tendencies as for the inner structures were found also for the outer rings (R), ringlenses (RL) and lenses (L) (Fig. 10d,e,f).

We conclude that although the sizes of bars, rings and lenses depend on the galaxy luminosity, the luminosity does not uniquely define their sizes. In barred galaxies, the size of the structure depends also on the Hubble type (smaller in the early-type S0s) and in non-barred galaxies the lenses are smaller in the most luminous galaxies.

6 DISCUSSION

Secular galaxy evolution is actively debated both from the observational and the theoretical points of view. Large galaxy surveys are under progress, focusing on this topic via galaxy morphology at different redshifts, largely based on automatic analysis approaches. However, it is also important to study the nearby galaxies, for which more detailed analysis can be made. Bars are expected to be important driving forces of secular evolution. They are efficient drivers of gas to the central regions of the galaxies (Shlosman, Frank & Begelman 1989; Shlosman, Begelman & Frank 1990), possibly adding mass to the bulge or even creating nuclear bars (Friedli & Martinet 1993). Bars can drive spiral arms (Salo et al. 2010 and references there) or they can be in the dynamical interaction with the haloes (Athanassoula 2003; Martinez-Valpuesta, Shlosman & Heller 2006) as well as with the bulges (Athanassoula & Misioritis 2002; Athanassoula 2003; Saha, Martinez-Valpuesta & Gerhard 2012), leading to re-distribution of stellar matter in galaxies. In
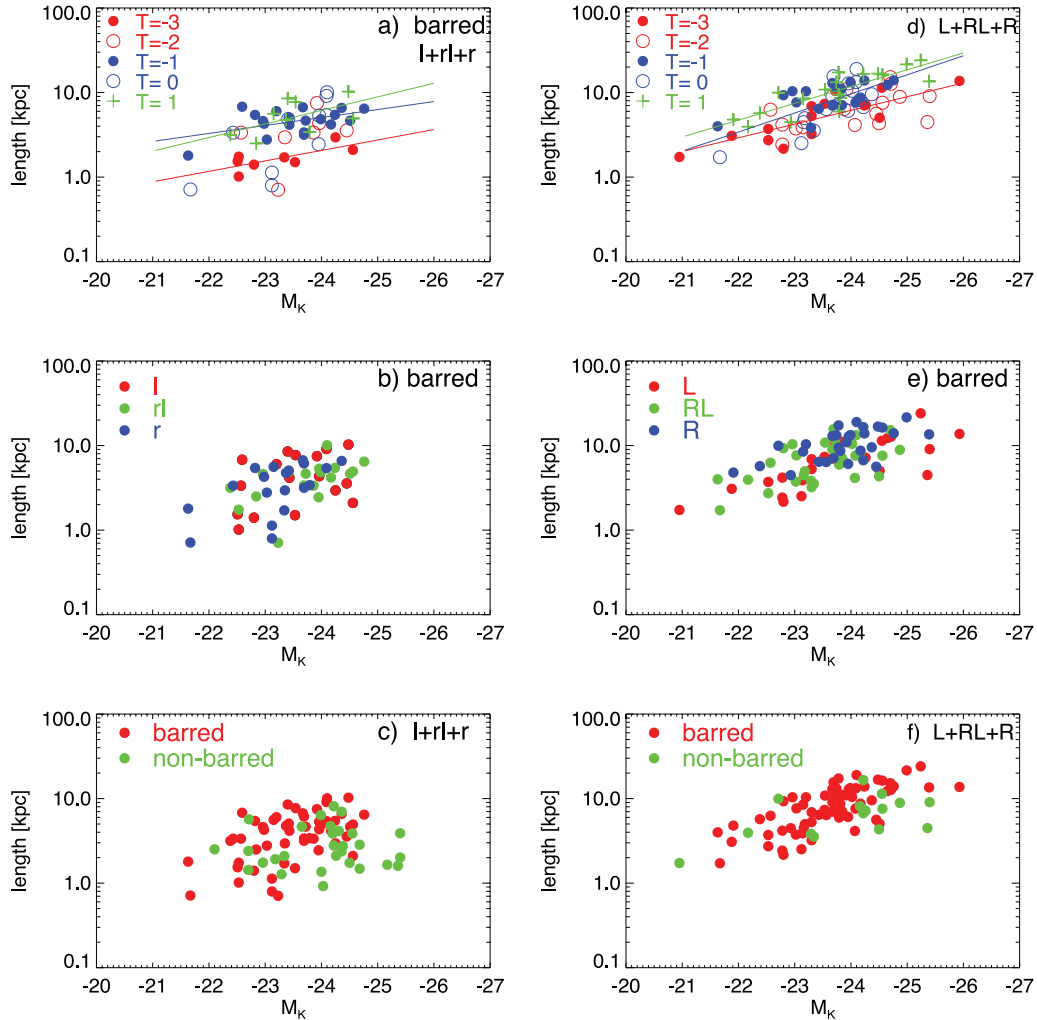
Figure 10. The lengths of outer rings, ringlenses and rings are shown as a function of galaxy brightness. The lengths are given in kiloparsecs.

the following possible manifestations of secular evolution in the morphology of the S0 galaxies are discussed.

6.1 Do bars induce bulge growth?

The fact that the bulges in S0s are on average fairly exponential ($\langle n \rangle \sim 2$) is consistent with the idea that many of them are (or contain) pseudo-bulges (or in terminology of Athanassoula 2005, discy bulges) triggered by bars. However, the result that the B/T flux-ratio is smaller in the strongly barred S0s (compared to weakly barred or non-barred S0s), is seemingly in contrast with bar-induced bulge growth, because strong bars are expected to be more efficient drivers of gas to the central regions of the galaxies (Shlosman et al. 1989, 1990).

Nevertheless, there is an alternative point of view. Galaxies that have relatively small (non-classical) bulges have slowly rising rotation curves, provided that their dark matter halo is not too centrally concentrated or cuspy). In that case, no Inner Lindblad Resonance (ILR) barrier is expected for inward moving trailing perturbation wave packets, which can thus reflect from the galaxy centre as fresh leading packets (Toomre 1981; Salo & Laurikainen 2000; see also review by Athanassoula 1984). If the disc is reactive (low value of Toomre Q parameter), this may lead to an efficient swing amplification cycle (Toomre 1981) and a strong secular bar growth (Athanassoula 2012). Because of its strength, such a bar will eventually lead to a growth of a relatively massive pseudo-bulge, but since the galaxy will have no classical bulge its B/T flux-ratio will remain small. On the other hand, galaxies which initially have a massive (or classical) bulge have a more steeply rising rotation curves, implying an ILR for all small to intermediate large pattern speeds, likely to inhibit bar formation or allow only weak bars to grow. Therefore, it is possible that the bulges we observe in strongly barred galaxies were induced by bars, whereas the bulges in weakly barred systems were largely formed at the epoch prior to bar formation. In this context, the recent observations by Pérez et al. (2011) are interesting because they have shown that the bulges in barred early-type galaxies are more metal rich and more α enhanced than the bulges of their non-barred counterparts. This indicates that the bulges of typical barred galaxies were formed later than the bulges of non-barred galaxies, possibly in a rapid starburst.

Disc-like pseudo-bulges form also in cosmological simulations due to massive starbursts at high redshifts, without invoking any secular evolution (Okamoto 2013). These bulges can be maintained up to the redshift zero, in case that the galaxies have not had any subsequent merger events with mass ratios larger than 0.1. However, such simulated bulges are generally more massive than the observed bulges, both in spirals and in S0s (Governato et al. 2007; Scannapieco et al. 2011).

6.2 Do main bars trigger nuclear bars?

There are two main types of *N*-body simulations producing long-lived nuclear bars: those in which the initial conditions of the simulations include a specific inner component, be it a disc or a pseudo-bulge, whose instability could form an inner bar (Friedli & Martinet 1993; Debattista & Shen 2007; Shen & Debattista 2009) or those in which the nuclear bar forms spontaneously from standard initial conditions (Heller, Shlosman & Englmaier 2001; Rautiainen, Salo & Laurikainen 2002; Englmaier & Shlosman 2004; Heller, Shlosman & Athanassoula 2007a,b). It is, however, still an open question, as well as one that needs to be observationally tested, what physical

conditions in galaxies are necessary in order to create long-lasting double bars.

Double bars appear in 20 per cent of the disc galaxies (Laine et al. 2002; Erwin & Sparke; Laurikainen et al. 2009; this study) and therefore are hard to understand merely as transient features in galaxies, as suggested based on the early simulations by Friedli & Martinet (1993) and Englmaier & Shlosman (2004). In this study, we have additionally shown that nuclear bars appear more frequently among the weakly barred (AB) than among the strongly (B) barred galaxies (44 per cent and 24 per cent, among the AB and B families, respectively).

From the point of view of our observations, the theoretical models by Maciejewski & Athanassoula (2008) are the most interesting. In their models both the nuclear and the main bar are supported by loops, equivalent to periodic orbits, but for the case of double rather than single bars (the terminology of loops is from Maciejewski & Sparke 1997). Maciejewski and Athanassoula found that the most stable models are those in which the main bar is not too massive and/or the ellipticity of the bar is not very high (their models 16 and 17), thus diminishing the fraction of phase space with chaotic orbits. This kind of bars are very much like the AB family of bars, which in this study are found to have a large number of nuclear bars.

An important question is also why do we see nuclear-sized bars in galaxies without any main bar. Such galaxies in our sample are: NGC 484, NGC 1553, NGC 2902, NGC 3169, NGC 3998, NGC 4694 and NGC 5333, including the faint bars detected only in the residual images. Characteristic for these galaxies is that they are often luminous and have quite large B/T flux-ratios ($\langle B/T \rangle = 0.44 \pm 0.06$) and relatively large values of the Sérsic index ($\langle n \rangle = 2.6 \pm 0.2$). The values are similar or even larger than those in the early-type S0s (for $T = -3$ $\langle B/T \rangle = 0.39$ and $\langle n \rangle = 2.2$), and significantly larger than for the late-type S0s (see Laurikainen et al. 2010: for $T = -1$ $\langle B/T \rangle = 0.28$ and $\langle n \rangle = 2.1$). A possible reason why the nuclear-sized bars in the 'non-barred' galaxies are so small might be related to the impact of the massive bulges to the rotation curves, which not only make it harder to create bars (as discussed in Section 6.1), but also make the bars smaller. This is because of their higher bar pattern speeds (must exceed the maximum of $\Omega - \kappa/2$), which implies shorter co-rotation distances, and therefore also shorter bars.

6.3 Formation of lenses in barred S0s

In his pioneering paper, Kormendy (1979) suggested that lenses in barred galaxies form when the stars in bars are gradually spilled out, forming more axisymmetric structures surrounding the bar. In this picture, the inner lenses are expected to have similar dimensions as the bars. The similarity of the lengths of bars and bar-related inner structures was shown by Kormendy in the optical region for a large range of Hubble types, including the S0s. He also concluded that the galaxy mass (luminosity) uniquely defines the sizes of bars and of all the structures related to bars.

However, in this study we found that the fully developed lenses are on average a factor of 1.3 larger than the bar. We also showed that in the near-IR the galaxy luminosity does not uniquely define the sizes of bars and the bar-related structures: the size depends also on galaxy morphology (smaller in the early-type S0s with $T = -3, -2$). Therefore, our observations do not give any clear support to the mechanism suggested by Kormendy (1979).

Lenses in barred galaxies form also in the simulation models by Athanassoula (1983), most likely via disc instability in a similar
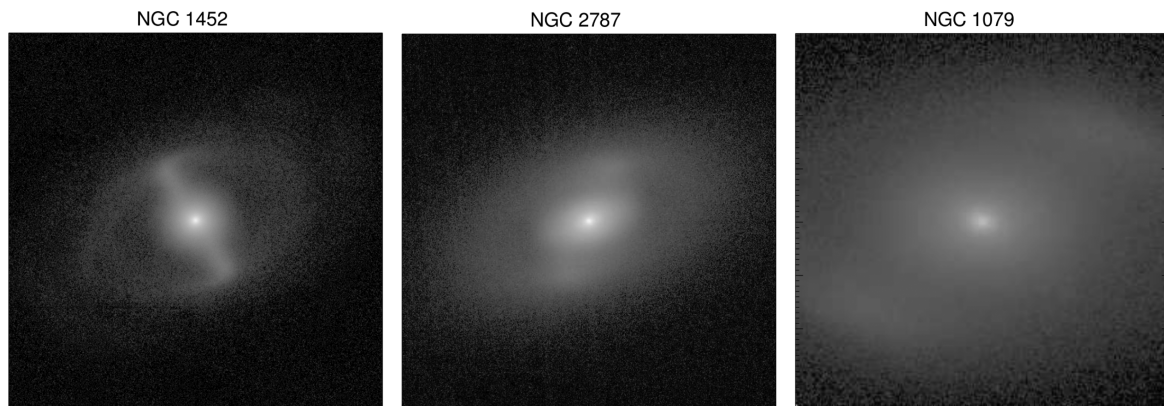
Figure 11. Examples of barred galaxies: (a) NGC 1452 has as classical bar + ring, (b) in NGC 2787 most of the light of the bar is concentrated to ansae and (c) in NGC 1709 the ansae of the bar look like starting to dissolve into the ring.

manner as bars. As the main difference between bars and lenses is in the ellipticity, in her models the lens formation can be accounted for by a larger amount of random motions initially present in the disc, e.g. the disc is dynamically hot. If both cool and hot components are present, a bar and a lens can appear in the same galaxy with the same orientations and lengths. Thus, the factor of 1.3 difference in the observed sizes of bars and inner lenses can be a problem also in her models.

Lenses in some barred galaxies might also be resonance-related structures, formed by dynamical heating from rings, which are gradually transformed into lenses via a ringlens phase (Buta 1995; Laurikainen et al. 2011). It is easy to find pictorial examples of such possible evolution (see Fig. 11), but we also have other observational evidence supporting this hypothesis. We showed that the mean ratio for the lengths of the outer (L, RL) and inner (l, rl) lenses is ∼1.9, which is very close to that obtained for the outer and inner rings (ratio ∼2.0) (Kormendy 1979; Athanassoula et al. 1982; Buta 1995). In the linear resonance theory, the predicted-length ratio for the Outer Lindblad Resonance (OLR) and the Corotation Radius (CR) is $length(\text{OLR})/length(\text{CR}) = 1 + \sqrt{2}/2 \sim 1.7$, for a flat rotation curve. According to typical slopes of the rotation curves of Sa−Sb galaxies, the predicted range is between 1.7 and 2.3 (Athanassoula et al. 1982). The fact that the rings and ringlenses appear in the same Hubble types (see Fig. 12) is consistent with this picture. However, the fully developed lenses are clearly more common in the early-type S0s, and have a larger length difference between the outer and inner components than in case of the rings. This implies that not all lenses can be formed via a ringlens phase.

6.4 Lenses in the non-barred S0s: relics of partially dissolved bars?

In the scenario by Kormendy (1979), the lenses in the non-barred galaxies are the end products of the transformation process, e.g. all the stars of the bar have been eventually spilled out into a lens. Other suggestions for the formation of lenses in the non-barred galaxies are those given by Athanassoula (1983) and Bosma (1983). In the models by Athanassoula, it would mean that the galaxy is dynamically too hot for creating bars, but still cool enough for lens formation. Bosma (1983) showed first observational evidence that lenses in the non-barred galaxies are dynamically distinct from the outer discs. As the lenses were redder than the discs, he suggested that the primary components formed relatively early in the Universe by truncated star formation. Lenses may also form via ringlenses

or by winding of the spiral arms in the local Universe (Laurikainen et al. 2011). However, none of these scenarios can readily explain the formation of multiple lenses, or in particular why the inner lenses in the non-barred S0s are as small as those found in this study.

We find the normalized sizes of the inner lenses in the non-barred galaxies to be surprisingly similar to the sizes of barlenses in the barred galaxies: the sizes of both structures peak at $length/R_{25} = 0.2R_{25}$ (see Fig. 7c). This allows us to speculate that the inner lenses in the non-barred S0s might actually be former barlenses in galaxies in which the outer bar component has disappeared, possibly during the bar evolution. The typical dimensions of these structures are illustrated in Fig. 13, comparing in the same scale a barred galaxy with a barlens (NGC 1452) and a non-barred galaxy with an inner lens (NGC 524). This hypothetical partial bar destruction phase could be related to a sequence of ansae morphology: from pointy to more and more azimuthally dispersed appearance. Although there is no theoretical explanation for this (see the review by Athanassoula 2012), it is possible to find tentative examples of galaxies, in which such a process might be under progress. For example, in NGC 1079 it looks like the ansae had already started to disperse into the surrounding inner ring (see Fig. 11). On the other hand, there exist also barred galaxies with barlenses in which the ansae underfill the inner ring (NGC 7098).

NGC 524 is one of the brightest galaxies in NIRS0S, having both nuclear, inner and outer lenses. The normalized size of the inner lens is 0.2 R_{25}. NGC 524 has been recently studied spectroscopically by Katkov et al. (2011) covering a radial extent of ∼30 arcsec. Within this region, in our morphological classification (NIRS0S Atlas) we detect the small bulge at $r < 10$ arcsec and the inner lens at $r \sim 25$ arcsec. The nuclear lens inside the bulge has a dimension of $r \sim 6.5$ arcsec. The outer lens at $r \sim 57$ arcsec was not covered by Katkov et al. We can see that both the bulge and the inner lens of NGC 524 have very old stellar populations (>15 and 14 Gyr, respectively) and nearly solar metallicities. Similar old stellar populations of the bulges and discs in some other S0s have been detected by Sílchenko (2011), and for bars in S0s and spirals by Sánchez-Blázquez et al. (2011) and Lorenzo-Cáceres et al. (2012). The fact that the ages of the stellar populations of bars and lenses are so similar (at least in the galaxies studied so far) is consistent with the idea that the inner lenses in the non-barred galaxies are partially destroyed bars, e.g. are former barlenses. However, the observed stellar populations would be consistent also with the alternative suggestions by Kormendy (1979), Athanassoula (1983) and Bosma (1983).
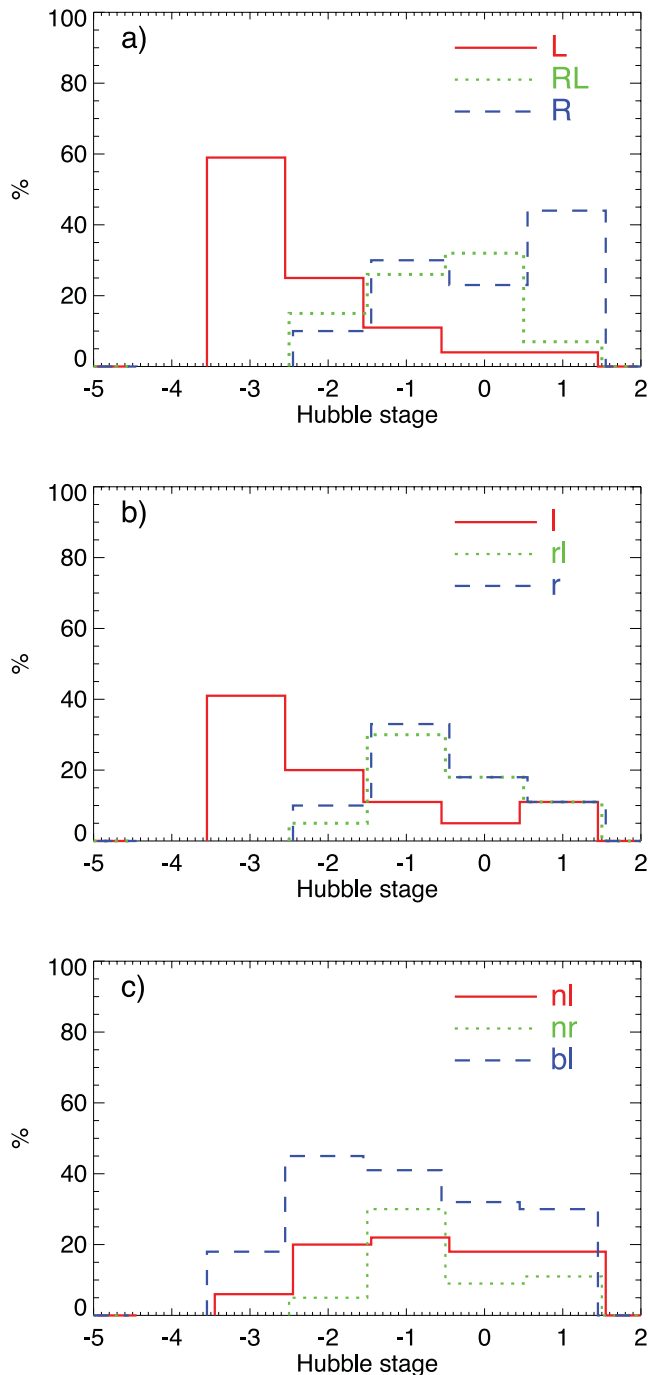
Figure 12. Fractions of the outer, inner and nuclear features are shown as a function of Hubble type. The different panels show the outer (a), inner (b) and nuclear (c) components.

6.5 Do S0s with different luminosities also have different formative processes?

Such a dichotomy for the S0s was suggested by Barway et al. (2007), using the galaxy magnitude $M_K = -24.5$ as a dividing line. The suggestion was based on the argument that the luminous and less-luminous galaxies have opposite trends in the scaling relation between the scale length of the disc (h_R) and the effective radius of the bulge (r_{eff}). However, in NIRS0S, using a few magnitudes deeper images and a much larger sample of S0s, such a dichotomy was not found (Laurikainen et al. 2010). It is also worth noting that

in Barway et al. the galaxies in both luminosity bins have Sérsic indexes larger than 3.2, indicating that the bulges in none of the two groups are pseudo-bulges in terms of having small Sérsic indexes. In Barway et al. two-component bulge-disc decompositions were made, while we used a multicomponent approach, allowing also fitting of bars and lenses.

However, the galaxy luminosity difference of 0.6 mag between the strongly barred and non-barred galaxies observed in this study (see also van den Bergh 2012; Barway et al. 2009) is real. In van den Bergh (2012, calculated for NIRS0S galaxies), it was partly attributed to large uncertainties in galaxy classifications between Sandage, de Vaucouleurs and us. However, a comparison of NIRS0S classifications with those in RSA and RC3 shows that the Hubble stage in NIRS0S generally agrees with that given by Sandage, because in both studies special attention was payed to the identification of lenses (which were largely ignored by de Vaucouleurs). On the other hand, bar classifications in the NIRS0S Atlas are more consistent with those given in RC3: the galaxies classified as AB by us and by de Vaucouleurs are typically non-barred in RSA (the weak AB bar category is lacking in RSA). Therefore, we don't see any major classification problem in NIRS0S.

It is clear that the bright non-barred S0s cannot be merely stripped spirals in which the star formation has been ceased. Aguerri, Balcells and Peletier (2001) and Eliche-Moral et al. (2012) showed that dry intermediate and minor mergers can induce bulge growth so that a galaxy with S0c morphological type can develop into S0b and S0b into S0a, without significantly increasing the Sérsic index of the bulge. This is consistent with the observed B/T flux-ratios in S0s, including some very small values, forming part of the parallel sequence of S0s and spirals (Laurikainen et al. 2010; Kormendy & Bender 2012). However, bulges in the S0$^-$ galaxies ($\langle B/T \rangle \sim 0.39$) are on average more massive than in the early-type spirals which is difficult to account for by minor mergers alone, particularly because the galaxies in NIRS0S appear mostly outside dense galaxy clusters. On the other hand, if these galaxies were formed by major mergers, the fairly small Sérsic indexes ($\langle n \rangle \sim 2.2$, see Laurikainen et al. 2010) and the large number of lenses in the very early type S0s (among $T = -3$ even 30 per cent have inner and outer lenses) would be difficult to explain. Alternatively, the most luminous non-barred galaxies were formed first and also evolved more rapidly (Cowie et al. 1996).

It is worth noticing that in the current study fairly bright galaxies have been discussed. It is still possible that the lower luminosity S0s, near the borderline to the dwarf early-type galaxies (dEs), were formed in a different manner (see Barazza et al. 2008; Kannappan, Guie & Baker 2009). The structures of dEs, based on multicomponent decompositions, have been recently studied by Janz et al. (2012).

7 SUMMARY AND CONCLUSIONS

The fractions of structural components and their dimensions are studied using NIRS0S, which is a magnitude ($m_B \leq 12.5$ mag) and inclination-limited (less than 65°) sample of ~200 early-type disc galaxies, including 160 S0+S0/a galaxies. We use the morphological classifications and the measurements of the dimensions of bars, rings, ringlenses and lenses, given in the NIRS0S Atlas (Laurikainen et al. 2011), after first converting them to the plane of the galactic disc. The dust-corrected properties of the bulges are taken from Laurikainen et al. (2010), based on two-dimensional multicomponent structural decompositions. To our knowledge, this
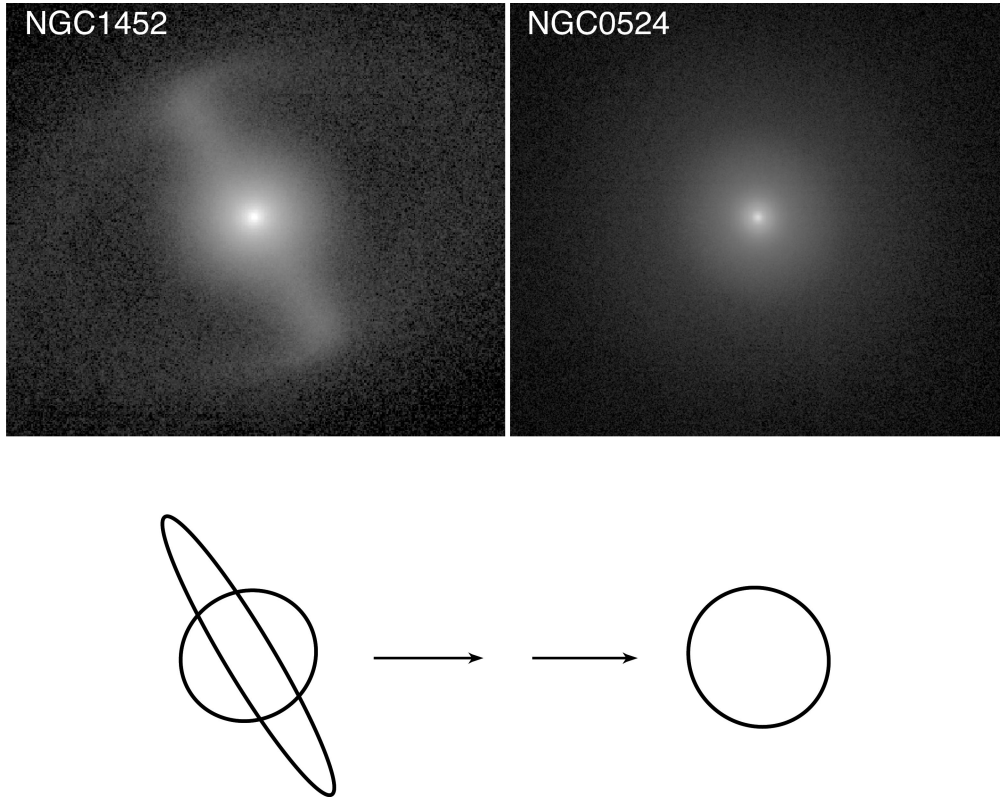
Figure 13. A tentative example illustrating a possible bar dissolution process. Upper-left panel: NGC 1452 has a bar and a barlens inside the bar. Upper-right panel: NGC 524 has nuclear, inner and outer lenses, but no bar. Lower panels: a schematic illustration of the dissolution process. In the left-hand panel the elongated component and the circle are shown in the same scale as the bar and the barlens in NGC 1452. In the right-hand panel the circle corresponds to the inner lens of NGC 524, drawn in the right-hand scale.

is the first statistical study of the multiple structure components of the S0s particularly focusing on lenses.

Our main conclusions are the following.

(1) *Lenses in barred galaxies.* Inner lenses (l) in barred S0s are found to be on average a factor of 1.3 larger than the bars (Fig. 6b). This is not consistent with the formative processes of lenses suggested by Kormendy (1979) and Athanassoula (1983), which favour similar dimensions for bars and lenses. On the other hand, inner rings (r) and ringlenses (rl) have similar sizes as bars. In barred multiple-lens systems, we find observational evidence of the resonant nature of the lenses: $length(L, RL)/length(l, rl) = 1.9 \pm 0.2$, which is similar to the outer and inner rings$(length(R)/length(r)) \sim 2$, generally associated with the known resonances of the rotating bar or linked to resonances via bar-driven manifolds.

(2) *Inner lenses in the non-barred S0s: barlenses in former barred galaxies, in which the outer bar component has been destroyed.* The normalized sizes of the inner lenses (l) in the non-barred galaxies are found to have similar sizes as barlenses (bl) in barred galaxies, peaked at $length/R_{25} = 0.2R_{25}$. As an example, we discuss NGC 524, which is one of the brightest galaxies in our sample and in which galaxy the lens contains similar old stellar population (Katkov et al. 2011) as bars in some observed S0s and early- and intermediate type spirals.

(3) *Inner lenses in the family classes.* The fractions are found to be nearly constant, being 21 ± 4 per cent, 21 ± 5 per cent and 16 ± 4 per cent in A, AB and B families, respectively. In the non-barred galaxies, the fraction of inner lenses is enhanced in respect of all the other structure components.

(4) *Main bars.* The bar fraction gradually drops from the Sa−S0/a galaxies (80 per cent have bars) towards the S0$^-$ types (35 per cent have bars). The B/T flux-ratio is smaller in the strongly barred (B) than in the weakly barred (AB) or non-barred (A) S0s. Bulges in the strongly barred S0s are interpreted to be triggered by bars, whereas in the weakly barred systems they are suggested to have formed in cumulative accretion events prior to the bar formation.

The mean semi-major axis length of the main bars is ∼4 kpc, with no difference in size between the single and double-barred galaxies (4.1 ± 0.4 kpc versus 4.4 ± 0.4 kpc, respectively). The mean size of the nuclear bars is 0.7 ± 0.4 kpc (0.1–1.5 kpc). The sizes of nuclear bars in non-barred galaxies were found to cover the range 0.3–0.9 kpc.

(5) *Barlenses, manifestations of evolved bars.* Barlenses are typically embedded in the inner parts of those bars that have ansae at the two ends of the bar (ansae exist in 52 ± 9 per cent versus 24 ± 6 per cent of barred galaxies with and without barlenses, respectively), which ansae in the simulation models (Athanassoula & Misioritis 2002) are associated with evolved bars. The frequency of barlenses does not depend on the galaxy brightness (31 ± 5 per cent versus 32 ± 7 per cent in the two galaxy luminosity bins, respectively). Also, multiple lenses are rare in the galaxies with barlenses (24 ± 2 per cent versus 56 ± 6 per cent in barred galaxies with and without barlenses, respectively).

(6) *Nuclear bars.* Contrary to the previous results, we find that nuclear bars appear more frequently in the weakly barred (AB) than in the strongly barred (B) galaxies (44 ± 8 per cent versus 24 ± 6 per cent among the AB and B galaxies, respectively), which is consistent with the theoretical models by Maciejewski & Athanassoula (2008).

Contrary to the main bars, nuclear bars (+ nuclear lenses) appear in a similar manner in all Hubble types in NIRS0S (until the fraction drops at $T = -3$).

Nuclear-sized single bars are detected in seven 'non-barred' galaxies. The small sizes of the bars are explained due to the large bulges of these galaxies: they might have prevented the formation of larger bars, due to the high $\Omega - \kappa/2$ barrier for the bar pattern speed, placing the co-rotation fairly close to the galaxy centre.

(7) *Does the formation of the structure depend on the galaxy luminosity?* The family classes A, AB and B cover the same galaxy luminosity range, but the mean luminosity gradually decreases from A → AB → B, so that the non-barred galaxies are on average 0.6 mag more luminous than the strongly barred galaxies. However, there is no upper limit in galaxy luminosity for bar formation. Also, galaxy luminosity does not uniquely define the sizes of bars or the structures related to bars.

ACKNOWLEDGEMENTS

REFERENCES

Aguerri J. A. L., Balcells M., Peletier R. F., 2001, A&A, 367, 428
Aguerri J. A. L., Méndez-Abreu J., Corsini E. M., 2009, A&A, 495, 491
Athanassoula A., ed., 1983, Proc. IAU Symp. 100, Internal Kinematics and Dynamics of Galaxies. Reidel, Dordrecht, p. 243
Athanassoula E., 1984, Phys. Rep., 114, 319
Athanassoula E., 2003, MNRAS, 341, 1179
Athanassoula E., 2005, MNRAS, 358, 1477
Athanassoula E., 2012, in Falcon-Barroso J., Knapen J. H., eds, Secular Evolution of Galaxies. Cambridge Univ. Press, Cambridge, preprint (arXiv:1211.6752)
Athanassoula E., Bosma A., 1985, ARA&A, 23, 147
Athanassoula E., Misioritis A., 2002, MNRAS, 330, 35
Athanassoula E., Bosma A., Creze M., Schwarz M. P., 1982, A&A, 107, 101
Athanassoula E., Romero-Gómez M., Bosma A., Masdemont J. J., 2010, MNRAS, 407, 1433
Barazza F. D., Jogee S., Marinova I., 2008, ApJ, 675, 1194
Barway S., Kembhavi A., Wadadekar Y., Ravikumar C. D., Mayya Y. D., 2007, ApJ, 661, 37
Barway S., Wadadekar Y., Kembhavi A. K., Mayya Y. D., 2009, MNRAS, 394, 1991
Barway S., Wadadekar Y., Kembhavi A. K., 2011, MNRAS, 410, 18
Bosma A., 1983, in Athanassoula E., ed., Proc. IAU Symp. 100, Internal Kinematics and Dynamics of Galaxies. Reidel, Dordrecht, p. 253
Buta R., 1995, ApJS, 96, 39
Buta R., 2013, in Oswalt T. D., Keel W. C., eds, Planets, Stars and Stellar Systems. Vol. 6: Extragalactic Astronomy and Cosmology. Springer, Berlin, p. 1
Buta R., Combes F., 1996, Fundam. Cosm. Phys., 17, 95
Buta R., Corwin H. G., Jr, Odewahn S. C., Langley J., Smith J., 2007, in Buta R. J., Corwin H. G., Odewahn S. C., eds, The de Vaucouleurs Atlas of Galaxies. Cambridge Univ. Press, Cambridge, p. 344

Buta R. et al., 2010, ApJS, 190, 147
Cappellari M. et al., 2011, MNRAS, 416, 1680
Coelho P., Gadotti D. A., 2011, ApJ, 743, 13
Comerón S., Knapen J. H., Beckman J., Laurikainen E., Salo H., Martínez-Valpuesta I., Buta R., 2010, MNRAS, 402, 2462
Conselice C. J., Bershady M. A., Jangren A., 2000, ApJ, 529, 886
Cowie L. L., Songaila A., Hu E. M., Cohen J. G., 1996, AJ, 112, 839
de Vaucouleurs G., de Vaucouleurs A., Corwin H. G., Buta R., Paturel G., Fouqué P., 1991, Third Reference Catalogue of Bright Galaxies. Springer, New York (RC3)
de Vaucouleurs G., de Vaucouleurs A., Corwin H. G., 1976, Second Reference Catalogue of Bright Galaxies. University of Texas Press, Austin (RC2)
Debattista V. P., Shen J., 2007, ApJ, 654, 127
Eliche-Moral M. C., González-García A. C., Aguerri J. A. L., Gallego J., Zamorano J., Balcells M., Prieto M., 2012, A&A, 547, 48
Englmaier P., Shlosman I., 2004, ApJ, 617, 115
Erwin P., 2004, A&A, 415, 941
Erwin P., 2005, MNRAS, 364, 283
Erwin P., 2011, Mem. Soc. Astron. Ital. Suppl., 18, 145
Erwin P., Sparke L., 2002, AJ, 124, 65
Frenk C. S., White S. D. M., Efstathiou G., Davis M., 1985, Nat, 317, 595
Friedli D., Martinet L., 1993, A&A, 277, 27
Governato F., Willman B., Mayer L., Brooks A., Stinson G., Valenzuela O., Wadsley J., Quinn T., 2007, MNRAS, 374, 1479
Graham A., Worley C. C., 2008, MNRAS, 388, 1708
Grouchy R., Buta R., Salo H., Laurikainen E., 2010, AJ, 139, 2465
Hammer F., Flores H., Puech M., Yang Y. B., Athanassoula E., Rodrigues M., Delgado R., 2009, A&A, 507, 1313
Heller C., Shlosman I., Englmaier P., 2001, ApJ, 553, 661
Heller C. H., Shlosman I., Athanassoula E., 2007a, ApJ, 657, L65
Heller C. H., Shlosman I., Athanassoula E., 2007b, ApJ, 671, 226
Holmberg E., 1975, in Sandage A., Sandage M., Kristan J., eds, Galaxies and the Universe, Vol. IX. The University of Chicago Press. Chicago, London, p. 154
Hopkins P. F., Kerés D., Ma C., Quataert E., 2010, MNRAS, 401, 1131
Janz J. et al., 2012, ApJ, 745, 24
Just D. W., Zaritsky D., Tran K. H., Gonzalez A. H., Kautsch S. J., Moustakas J., 2011, ApJ, 740, 54
Kannappan S., Guie J., Baker A., 2009, AJ, 138, 579
Katkov I., Chilingarian I., Sílchenko O., Zasov A., Afanasiev V., 2011, Balt. Astron., 20, 453
Keselman J. A., Nusser A., 2012, MNRAS, 424, 1232
Khochfar S. et al., 2011, MNRAS, 417, 845
Kormendy J., 1979, ApJ, 227, 714
Kormendy J., Bender R., 2012, ApJS, 198, 2
Kormendy J., Kennicutt R., 2004, ARA&A, 42, 603
Kraljic K., Bournaud F., Martig M., 2012, ApJ, 757, 60
Laine S., Shlosman I., Knapen J. H., Peletier R. F., 2002, ApJ, 567, 97
Laurikainen E., Salo H., Buta R., Vasylyev S., 2004, MNRAS, 355, 1251
Laurikainen E., Salo H., Buta R., Knapen J. H., 2005, MNRAS, 362, 1319
Laurikainen E., Salo H., Buta R., Knapen J. H., Speltincx T., Block D., 2006, AJ, 132, 2634
Laurikainen E., Salo H., Buta R., Knapen J. H., 2007, MNRAS, 381, 401
Laurikainen E., Salo H., Buta R., Knapen J. H., 2009, ApJ, 692, 34
Laurikainen E., Salo H., Buta R., Knapen J. H., Comerón S., 2010, MNRAS, 405, 1089
Laurikainen E., Salo H., Buta R., Knapen J. H., 2011, MNRAS, 418, 1452
Lorenzo-Cáceres A., Vazdekis A., Aguerri A. L. Corsini E. M., Debattita V. P., 2012, MNRAS, 420, 1092
Maciejewski W., Athanassoula E., 2008, MNRAS, 389, 545
Maciejewski W., Sparke L., 1997, ApJ, 484, L117
Martig M., Bournaud F., Croton D. J., Dekel A., Teyssier R., 2012, ApJ, 756, 26
Martinez-Valpuesta I., Shlosman I., Heller C., 2006, ApJ, 637, 214
Méndez-Abreu J., Simonneau E., Aguerri J. A. L., Corsini E. M., 2010, A&A, 521, 71
Nair P. B., Abraham R. G., 2010a, ApJ, 714, 260

Nair P. B., Abraham R. G., 2010b, ApJS, 186, 427

Navarro J., Benz W., 1991, ApJ, 380, 320

Okamoto T., 2013, MNRAS, 428, 718

Pérez I., Sánchez-Blázquez P., Zurita A., Florido E., 2011, in Carignan C., Freeman K., Combes F., eds, Proc. IAU Symp. 277, Tracing the Ancestry of Galaxies. Cambridge Univ. Press, Cambridge, p. 166

Puech M., Hammer F., Hopkins P. F., Athanassoula E., Flores H., Rodrigues M., Wang J. L., Yang Y. B., 2012, ApJ, 753, 128

Rautiainen P., Salo H., Laurikainen E., 2002, MNRAS, 337, 1233

Saha K., Martinez-Valpuesta I., Gerhard O., 2012, MNRAS, 421, 333

Sales L. V., Wang W., White S. D. M., Narvarro J. F., 2013, MNRAS, 428, 573

Salo H., Laurikainen E., 2000, MNRAS, 319, 393

Salo H., Laurikainen E., Buta R., Knapen J. H., 2010, ApJ, 715, 56

Sánchez-Blázquez P., Ocvirk P., Gibson B. K., Pérez I., Peletier R. F., 2011, MNRAS, 415, 709

Sandage A., 1961, The Hubble Atlas of Galaxies. Carnegie Institute of Washington, Washington, DC

Sandage A., Bedke J., 1994, The Carnegie Atlas of Galaxies. Carnegie of Institute Washington, Washington, DC

Scannapieco C., White S., Springel V., Tissera P., 2009, MNRAS, 396, 696

Scannapieco C., White S., Springel V., Tissera P., 2011, MNRAS, 417, 154

Schlegel D. J., Finkbeiner D. P., Davies M., 1998, ApJ, 500, 525

Sellwood J. A., Wilkinson A., 1993, Rep. Prog. Phys., 56, 173

Shen J., Debattista V. P., 2009, ApJ, 690, 758

Shlosman I., Frank J., Begelman M. C., 1989, Nat, 338, 45

Shlosman I., Begelman M. C., Frank J., 1990, Nat, 345, 679

Sílchenko O., 2011, in Tuffs R. J., Popescu C. C., eds, Proc IAU Symp. 284, The Spectral Energy Distribution of Galaxies. Cambridge Univ. Press, Cambridge

Skrutskie M. F. et al., 2006, AJ, 131, 1163

Toomre A., 1981, in Fall S. M., Lynden-Bell D., eds, The Structure and Evolution of Normal Galaxies. Cambridge Univ. Press, Cambridge, p. 111

Toth G., Ostriker J., 1992, ApJ, 389, 5

Tully R. B., 1988, The Nearby Galaxy Catalog. Cambridge Univ. Press, Cambridge

van den Bergh S., 1976, ApJ, 206, 883

van den Bergh S., 2012, ApJ, 745, 189

Wang J. et al., 2011, MNRAS, 413, 1373

Weinzirl T., Jogee S., Khochfar S., Burkert A., Kormendy J., 2009, ApJ, 696, 411

White S. D., Rees M. J., 1978, MNRAS, 183, 341

Wilman D. J., Oemler A., Jr, Mulchaey J. S., McGee S. L., Balogh M. L., Bower R. G., 2009, ApJ, 692, 298

This paper has been typeset from a TEX/LATEX file prepared by the author.